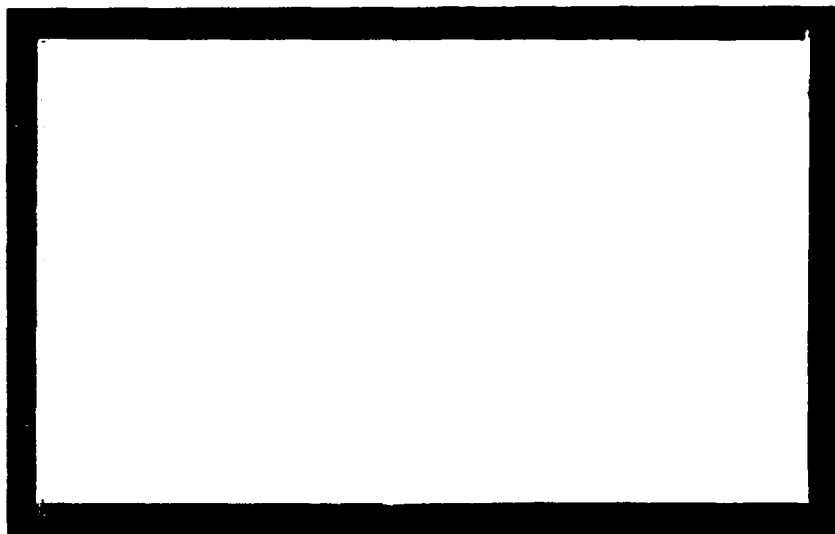




LEVEL

12

AD A 095567



FILE COPY

APPROVED FOR PUBLIC RELEASE;
DISTRIBUTION UNLIMITED

CENTER FOR MATERIALS RESEARCH

STANFORD UNIVERSITY • STANFORD, CALIFORNIA

81 2 26 050

12

9
Final Technical Report,
on
6
A FEASIBILITY STUDY ON THE GROWTH OF
BULK GaN SINGLE CRYSTALS.

Supported by NAVAIR

15 under
Contract N00019-79-C-0327

11 Jul 1980

14 CMR-80-13

12/63

Submitted by

Center for Materials Research
Stanford University
Stanford, CA 94305

Principal Investigator:
10
Professor W. A. Tiller
Materials Science and Engineering

Associate Investigators:
Professor R. S. Feigelson
Center for Materials Research

Dr. D. Elwell
Center for Materials Research

APPROVED FOR PUBLIC RELEASE;
DISTRIBUTION UNLIMITED

400 824

JP

TABLE OF CONTENTS

	<u>Page</u>
I. INTRODUCTION	1
II. BACKGROUND	4
III. EXPERIMENTAL DATA	10
IV. THEORETICAL MODEL	27
V. EXPERIMENTS TO BE DONE	36
VI. SUMMARY AND CONCLUSIONS	38
VII. REFERENCES	40

Accession for
NHS GRAM
DAG TMS
Unprocessed
Classification

By _____
Date _____
Approved _____

A

I. INTRODUCTION

Gallium nitride is probably the most interesting III-V semiconductor which has not yet been prepared in the form of large single crystals. It has a wide, direct bandgap (3.4 eV at 300K) and is potentially useful as an electroluminescent material and injection laser. The possibility of extending the laser frequency into the blue-green and blue regions is very attractive for underwater communication and other applications.

Some important properties of GaN are listed in Table I. Although a cubic zinc-blende phase has been mentioned in the literature (11), GaN normally crystallizes with the hexagonal wurtzite structure.

In addition to problems of growing large crystals, the practical applications of GaN are limited by the usual presence of a native donor of unknown origin which results in undoped material being n-type with a carrier concentration of $10^{18} - 10^{19} \text{ cm}^{-3}$ and a mobility in the region of $100 \text{ cm}^2 \text{ V}^{-1} \text{ s}^{-1}$. The highest value reported in the literature appears to be $440 \text{ cm}^2 \text{ V}^{-1} \text{ s}^{-1}$ (10). The material can be compensated by zinc to produce semi-insulating material (12) and compensation is also possible with Be, Li, and Mg. Doping with oxygen, dysprosium, cadmium, silicon, germanium, carbon, iron, and mercury has also been studied.

GaN has been made to lase in the ultraviolet (13) and to exhibit light emission over a wide spectral range. Reviews of its optical properties and luminescence have been published by Pankove and co-workers (11,14) and more recently by Jacob (15) who described blue electroluminescent devices with low operating voltage.

Most studies of the properties of GaN have been made on thin films deposited on sapphire by the vapor phase reaction between GaCl and NH_3 (1). In this study it was decided to adopt a different approach, in the hope both of producing bulk crystals and of reducing the concentration of native donors. Solution growth is normally more appropriate than vapor growth for the growth of bulk crystals, and gallium was chosen as a solvent because of purity considerations. So although the low solubility of GaN in gallium is a handicap, a feasibility study has been performed of solution growth as a method of producing

Table I: Properties of GaN

<u>Reference</u>		<u>GaN</u>
	Structure	wurtzite
	Lattice Constants	a = 3.189 c = 5.185
	Expansion Coefficients	
(1)	a direction (300°K to 1100°K)	$5.59(10)^{-6}/^{\circ}\text{K}$
	c direction (700°K to 900°K)	$3.17(10)^{-6}/^{\circ}\text{K}$
(2)	Bandgap energy (ev) at 2°K	3.477
	at 300°K	3.360
(2)	Bandgap Temperature Dependence (T 180°K)	$-6(10)^{-4}\text{ev}/^{\circ}\text{K}$
(3)	Bandgap Pressure Dependence: T=77°K	$(4.6 \pm .4)(10)^{-6}\text{ev}/\text{bar}$
	T=300°K	$(4.2 \pm .4)(10)^{-6}\text{ev}/\text{bar}$
(4)	Lowest Indirect Gap (2°K)	> 3.55ev
(5)	Heat of Formation (Kcal/mole)	26.4
(6)	Index of Refraction	2.5 ± 0.1
	Effective Masses:	
(7, 8)	Holes	0.8 ± 0.2
(7, 8)	Electrons	0.22 ± 0.03
(9)	Carrier Recombination Rate	$(3 \pm 2)(10)^7 \text{sec}^{-1}$
(10)	Electron Mobility (cm ² /volt-sec)	440

bulk crystals of GaN. Thermal gradient transport of dissolved GaN was thought, in principle, to be the most promising approach in view of the low solubility.

This report describes studies of the growth of GaN by the reaction between gallium and ammonia, in the presence of a carrier gas, usually hydrogen. Experiments on the growth of GaN in a horizontal chamber have been modestly successful in that they have shown that crystals over 2.5 mm long can be grown in 10 days. These experiments have identified the temperature and ammonia partial pressure conditions for relatively stable growth and have yielded useful insights into the growth process. Attempts to grow GaN by a vertical gradient transport technique and by the use of gallium/tin alloys have been much less successful. A theoretical model which explains most of the data pertaining to the growth of GaN by this method is included. Finally, recommendations are presented for further study, including suggestions of methods for growing large crystals which should be tried as a continuation to this study.

It should be emphasized that this was a short-term feasibility study so that long-term planning based on a detailed understanding of the system was not possible. The approach used was pragmatic and the numerical data was gathered as expeditiously as possible.

II. BACKGROUND

A. Stability of GaN

There is some controversy in the literature concerning the chemical and thermal stability of gallium nitride. Lorenz and Binkowski (16) found that thermal decomposition proceeds in vacuum at 600°C, and that dissociation is complete if prolonged heating takes place in nitrogen at 1000°C. Lyutaya and Bukanevich (17) reported decomposition of GaN in air at 700°C, by conversion to the oxide. Groh et al (18) studied thermal decomposition in vacuum and observed a small weight loss above 710°C but definitive decomposition only above 980°C. Our own experiments based on measurements of the pressure of gas evolved by GaN in a sealed, evacuated container showed that significant decomposition could be detected at 700°C and that the rate of decomposition at 1000°C was higher by an order of magnitude. The rate of decomposition was substantially unaffected by the presence of gallium.

Stability is enhanced by the presence of ammonia in the surrounding atmosphere, and also of nitrogen but only when the pressure is very high. Logan and Thurmond (19) reported that the rate of decomposition of GaN is small compared with the growth rate at an ammonia partial pressure roughly twice the equilibrium value, so long as the temperature was below 1050°C. Equilibrium pressure data for N₂ above GaN has been presented by Thurmond and Logan (2). This value is ~ 1000 atm at 1000°C and ~ 10⁵ atm at the melting point of ~ 1700°C. Equilibrium partial pressures of ammonia are much lower because of the greater tendency of NH₃ to dissociate into atomic nitrogen.

It has been suggested (21) that the gaseous decomposition product of gallium nitride is a polymeric molecule (GaN)_n at temperatures around 1000°C. However, the evidence for this hypothesis is poor and Schoonmaker et al (22) found by thermogravimetric and torsion effusion techniques that GaN decomposed at 900°C to Ga + N₂. This was confirmed by Groh et al. (18) who used a mass spectrometer to analyze the gaseous decomposition product and found only N₂.

B. Methods Used to Grow GaN

Table 2 lists the methods which have been used to grow GaN, excluding those which utilize the direct reaction between Ga and NH_3 which are considered in the next section. As was mentioned earlier, the most widely used method of preparing GaN has been to pass GaCl with NH_3 with purified hydrogen as carrier gas over a substrate, normally {0001} sapphire. The growth rate is typically $0.5 \mu\text{m}/\text{min}$ and most studies of the properties of GaN have been made on films prepared by variations of this method.

Silicon, silicon carbide, spinel, and gallium arsenide have also been tried as substrate materials as alternatives to sapphire (the GaAs at temperatures not exceeding 550°C), and dopants were introduced as volatile chlorides. Colorless films are said to be produced only if the hydrogen carrier gas is highly purified, for example by passing through a palladium diffusion furnace (39) or if purified helium is used as carrier gas.

Bulk crystals up to $25 \times 15 \times 5 \text{ mm}$ have been prepared using this technique (23) and have properties similar to those of the films. However, so far as we are aware, light emission has not been observed from bulk crystals grown in this way.

Alternative approaches include the use of nitrogen with GaCl at very high pressures (26), but the carrier mobility was lower than that obtained using $\text{GaCl} + \text{NH}_3$. The use of trimethyl gallium in place of GaCl also failed to give a lower native donor concentration or improved carrier mobility (28).

Sublimation has been used to give single crystals in the form of needles or platlets, typically up to $3\text{-}5 \text{ mm} \times 0.1 \text{ mm}$ in size (29-35). The authors agree that a temperature of $1150\text{-}1170^\circ\text{C}$ gives optimum results, with an ammonia flow typically of $100 \text{ cc}/\text{minute}$. No detailed characterization of crystals grown in this way appears to have been reported.

The use of nitrogen gas activated by rf, microwave or plasma to generate atomic nitrogen is an attractive alternative to the use of ammonia. So far, however, the experiments reported (36-38) have not

THIS PAGE IS BEST QUALITY PRACTICABLE
FROM COPY FURNISHED TO DDC

TABLE II. METHODS USED TO GROW GaN

Reference	Method	Ga Source	N Source	Carrier Gas	Reaction Zone Temperature (°C)	Reaction Zone Pressure	Substrate	Growth Rate mm/min	Crystal Size (max)	Crystal Color	Electrical Properties $\mu(\text{cm}^2/\text{V}-\text{s})^{-1}$	Comments
(1)	CVD	GaCl	NH ₃	H ₂	825	1 atm	{0001} Al ₂ O ₃	0.5	50-100 μm	colorless	1-5x10 ¹⁹	"classic" CVD paper
(2)	CVD	GaCl	NH ₃	H ₂ , He	1000-1200	1 atm	{110} Al ₂ O ₃ , GaN	10	25x15x5 mm	Dk green-colorless	~10 ¹⁹	better results with He
(3)	CVD	GaCl	NH ₃	He	1040-1060	1 atm	{0001} Al ₂ O ₃	0.5-1	-	colorless	1-2x10 ¹⁷	380
(4)	CVD	GaCl	NH ₃	H ₂ , He	600-1050	1 atm	{111} & {0001} Si	-	-	-	-	polycrystalline
(5)	CVD	GaCl	N ₂	-	650-840	40-130 Kbar	{110} Al ₂ O ₃	0.2-0.4	-	-	2-10x10 ¹⁹	30
(6)	CVD	Ga ₂ O	-	-	1000-1200	-	{110} Al ₂ O ₃	-	1-3mm needles	dark green	-	larger crystals dendritic
(7)	CVD	GaBr ₃ /NH ₃	complex	N ₂ , Ar, H ₂	600-750	1 atm	{111} Si; {0001} SiC	0.01-0.07	-	transparent	-	no deposition with H ₂
(8)	CVD	(CH ₃) ₃ Ga	NH ₃	He	700-1000	1 atm	{0001} Al ₂ O ₃ ; Si; {111} MgAl ₂ O ₄ ; {0001} SiC ^{2,4}	0.1	6 μm	yellow to red-brown	>10 ¹⁹	60
(9)	sublimation	GaN	NH ₃	-	1150-1200	1 atm	-	2	2mm	clear	-	hexagonal needles
(10)	sublimation	GaN	NH ₃	-	1150	1 atm	-	11	4x0.1 mm	-	-	hexagonal needles
(11)	sublimation	Ga ₂ O ₃ /GaN/Ga	NH ₃	-	1170	1 atm	-	0.1	3x0.5 mm	green	-	needles
(12)	sublimation	GaN	NH ₃	-	1150-1200	1 atm	-	1.2	5x1 mm	colorless	-	hexagonal needles
(13)	sublimation	Ga ₂ O ₃	NH ₃	-	600-1100	1 atm	-	-	-	pale yellow gray	-	dissociation as low as 600°C
(14)	sublimation	Ga ₂ O ₃	NH ₃	-	1150	1 atm	-	-	3x0.1	amber	-	0.5 μm platelets and needles
(15)	sublimation	GaAs-Ga ₂ O ₃	NH ₃	-	700-1200	1 atm	-	-	-	yellow	-	2-phase above 1100°C (Ga ₂ O ₃)
(16)	sublimation	GaP, GaAs	NH ₃	-	1000-1100	1 atm	-	-	-	yellow; white	-	white from GaAs
(17)	RF sputtering	Ga	N ₂	-	20-750	0.02 torr	{0001} Al ₂ O ₃ {111} Si	-	-	light yellow	-	polycrystalline films
(18)	reactive evaporation	Ga	activated N ₂	-	200-550+	-	{111} GaAs; {0001} Al ₂ O ₃	0.2-0.3	-	transparent	-	microvoid attenuation
(19)	plasma deposition	(CH ₃) ₃ Ga	NH ₃ , N ₂ , H ₂	-	300	0.15 torr	NaCl	3x10 ⁻⁴	1.5 μm	transparent pale yellow	-	polycrystalline
(20)	high pressure solution	Ga	NH ₃	-	940-1250	1.5-8 Kbar	{0001} Al ₂ O ₃	7x10 ⁻⁴	10 μm	-	10 ¹⁹	70

THIS DOCUMENT IS UNCLASSIFIED
DATE 08-11-2010 BY 10880

given really promising results and the growth rates reported in the plasma deposition process (38) are extremely low.

High pressure solution techniques with up to 8 kbar pressure reported by Madar et al. (39) appear promising in principle but again the electrical properties of materials produced by this method are not encouraging and we understand that this work has been discontinued.

C. Solution Growth

The previous experiments on the growth of crystals by reacting ammonia with liquid gallium are listed in Table 3. The earliest experiments were concerned with synthesis rather than crystal growth but those of Pichugin and Yaskov (40) yielded needles up to 5 mm long x 0.3 mm diameter, probably grown by sublimation and condensation during synthesis. The first careful study of this method as a means of growing high quality material was that of Logan and Thurmond (19). They grew epitaxial layers on {0001} sapphire using both Ga and Ga/Bi alloys by flowing ammonia in an H₂ carrier at temperatures in the range 850-1150°C. A temperature gradient across the melt was considered essential. The carrier concentration in the films was $\sim 10^{19} \text{ cm}^{-3}$ and the mobility of undoped films about $75 \text{ cm}^2 \text{ V}^{-1} \text{ s}^{-1}$.

Related experiments were performed by Ejder (42) who used nitrogen as carrier gas and tried to grow single crystals rather than epitaxial layers. His largest crystals were needles 5 mm long and a few microns in diameter, grown rather rapidly, and small needles were produced by Ogino and Aoki (33) using similar methods. Very recently the growth of epitaxial layers on sapphire and silicon carbide was reported by Vodakov et al (43), using pure ammonia rather than a carrier gas.

The main conclusions of the Logan and Thurmond study (19) are listed in Table 4. In summary, a temperature and partial pressure range for epitaxial growth was determined, and the use of bismuth and a temperature gradient were found beneficial for the growth of continuous layers. Our aim was to extend this work to grow bulk crystals, relying on the Logan and Thurmond observations with minimal emphasis on improving the fundamental data base.

Table 3. Crystal Growth of GaN from Ga + NH₃

Reference	Reaction zone temperature (°C)	NH ₃ flows rate (cc/min)	Carrier gas	Substrate	Growth rate (µm/min)	Crystal size (max)	Crystal color	Comments
(40)	800-1250	120	-	-	-	5mm x 300 µm	Transparent	Optimum temp 1150°C Needles and Plates
(41)	1050	-	-	-	-	1 µm	grey	Powder synthesis
(19)	850-1150	0.5	H ₂	{0001}Al ₂ O ₃	0.4	500 µm	grey/black	Better nucleation with Ga/Bi alloy
(42)	1000-1150	-	N ₂	-	7	5mm x few µm	-	Whiskers, needles, platlets, and prisms
(33)	1100-1200	-	-	-	-	100 µm	-	Needles
(43)	1100-1200	167-333	-	Al ₂ O ₃ SiC	-	-	-	Epitaxial layers

Table 4. Constraints in Growing GaN from Ga Solutions (19)

1. The equilibrium partial pressure p^* of NH_3 above GaN is $\sim 10^{-3}$ atm at 900°C .
2. At $p \gtrsim 2p^*$, the reaction proceeds rapidly and Ga tends to leave the crucible because it strongly wets a GaN film on the crucible wall.
3. At $T < 950^\circ\text{C}$, the reaction may be prevented by a thin surface film of GaN.
4. Explosive decomposition of GaN crystallites may occur, especially above 1000°C .
5. The solubility of GaN in Ga is very low, $\sim 3 \times 10^{-5}$ molar at 1150°C .
6. A temperature gradient is required for the deposition of large area epitaxial layers.
7. Bi addition reduces nucleation in the melt.

III. EXPERIMENTAL DATA

Our experiments over the two-year program were mainly in three categories:

- (1) Determination of the solubility of GaN in Ga.
- (2) Studies of the feasibility of growing large GaN crystals in a horizontal furnace with a temperature gradient.
- (3) Studies of temperature gradient growth of GaN in a vertical crucible.

We shall summarize these in turn, with emphasis on the horizontal furnace.

A. Solubility Determinations

We attempted to measure the solubility of GaN in Ga by a vacuum decomposition method. This consisted of (a) passing NH_3 with a carrier gas over gallium for a time long enough to form a saturated solution, but not a surface layer of GaN (typically one hour), (b) quenching to room temperature, (c) evacuating the space above the gallium solution and sealing off a small volume containing the sample and a pressure gauge, (d) heating the solution to 1000°C to decompose the GaN, and measuring the pressure as a function of time as N_2 gas was evolved. The vapor pressure of gallium is low in the temperature range considered and can be ignored in comparison with that due to evolved N_2 .

This method confirmed that the solubility is in the region indicated by Logan and Thurmond (19), namely $\sim 10^{-5}$ molar at 950°C , but reliable quantitative measurements were difficult. Particular problems were encountered with achieving really leak-proof seals, especially between silica and stainless steel, and with virtual leaks due to adsorption of the carrier gas, and resources were not available to construct a sophisticated system capable of accurate measurement.

In view of these problems, no measurements of solubility were attempted during the second year of this program. Neutron activation analysis and mass spectrographic analysis were considered as alternatives but commercial analytical laboratories would not undertake these determinations. It was considered that the most accurate solubility determinations could be obtained by the Kjeldahl method, in which the dissolved nitrogen is converted back to ammonia and determined by

titration, but again a commercial laboratory which would perform this experiment on one of our solutions could not be located.

B. Horizontal Gradient Growth

1. Experiments Using Vitreous Carbon Crucible

The use of a horizontal crucible was suggested by Logan and Thurmond (19) and our earliest experiments were performed using a vitreous carbon crucible 6" in length and located in a temperature gradient with limits of about 900° and 1000°C. A sapphire wafer was located either in the hot end or the cold end of the furnace and the boat was charged with about 50g of gallium or Ga/Bi alloy. The ammonia partial pressure was adjusted to a value in the region suggested by Logan and Thurmond, namely $1.5 - 2 \times 10^{-3}$, and the hydrogen flow rate was normally 200 cc/min. The gas lines were of stainless steel and silica only, except for brass components in the pressure regulator. At the time of the last annual report, the largest crystal which had been grown was about 400 μm long.

In contrast to the earlier work (19), the use of Ga/Bi alloys was found to result in a higher incidence of nucleation and smaller crystals than gallium alone. Especially since the effect of the bismuth on solubility and transport properties is uncertain, most of our studies over the last year have been made using pure gallium (99.9999% pure material from Alusuisse) as solvent.

Attempts were made to restrict nucleation by localized cooling. Initially Peltier cooling was used to define a cold spot by the passage of current between a pair of electrodes which just contacted the surface of the gallium. However, although a current of over 10 A cm^{-2} was passed between the electrodes, no growth of GaN was observed on either. Small crystallites did grow in these experiments on the walls of the silica crucible and even on the silica bridge in which the electrodes were located.

An alternative arrangement was used in which localized cooling was provided by a "cold finger," a graphite cone supported above the melt such that only its tip contacted the melt surface. The finger was

cooled by passing the hydrogen and ammonia through a tube to enter the hollowed-out center of the cone, from which it emerged via four radial holes. Again this arrangement was totally unsuccessful since GaN nucleated over all the melt surface, apparently independent of the cold finger. These experiments were the first to give GaN in the form of needles, which had been reported previously by Ejder (42) and Ogino and Aoki (33).

A series of experiments was performed with argon as carrier gas and with flow rates, experiment duration, and temperature gradients similar to those used for hydrogen. The argon was purified by passing over Ti chips at about 700°C. Argon was found to have an adverse effect on the growth morphology, since it led to the deposition of GaN only in the form of needles. Many of these needles were tipped with Ga, suggesting that they had grown by the VLS (vapor-liquid-solid) mechanism (Fig. 1). Several needles were found to be hollow.

The needle morphology was attributed to a high supersaturation arising from an argon flow rate which was substantially lower than that of hydrogen so that the partial pressure of NH_3 was higher.

It had been found in earlier experiments that GaN nucleates relatively easily on graphite. Nucleation on graphite wafers was therefore studied in one series of experiments, the subsidiary aim being to prepare coated wafers for use as source and seed in a vertical crucible. In these experiments hydrogen was used as carrier gas with the steepest temperature gradient, about 180°C across a six-inch crucible. Pure Ga was used as solvent, the hot end of the crucible being at 1010°C and the cold end at about 825°C, with the experiment proceeding for about ten days.

The best results were obtained with three wafers located respectively at the hot end, center, and cold end, resting across the top of the crucible. These wafers restricted the creeping of gallium toward the hot end of the furnace, an effect which depends on the high surface tension of gallium and is therefore influenced by temperature gradients and by the contacting surface. Crystals grown during this experiment

reached 1.5 mm in length.

The electrical conductivity of crystals about 1.5 mm long and 0.4 mm in diameter was measured by a two-contact method with an indium amalgam contact applied to each end. The measured conductivity along the c-axis was 1-5 $(\Omega\text{cm})^{-1}$, the higher value being more reliable. Typical material grown by other investigators had $n \sim 10^{19} \text{cm}^{-3}$ and $\mu \sim 10-10^2 \text{cm}^2 \text{V}^{-1} \text{s}^{-1}$, so that $\sigma \sim 20-200 (\Omega\text{cm})^{-1}$. The low value of conductivity of our crystals may be due to a lower defect concentration, or to a low mobility, but the method of measurement may underestimate the true conductivity by an order of magnitude because of the contact resistance.

An alternative means of studying growth and nucleation of GaN was by the use of a Transtemp gold-coated transparent furnace, initially to observe GaN crystallization in the same vitreous carbon boat used for earlier studies. The maximum operating temperature of this furnace is limited, because of gold evaporation, to a value below 1000°C and so the temperature of the hot end of the boat was set at 970°C. The temperature gradient was also lower, roughly one-fifth of that used in previous experiments, and the NH_3 partial pressure was about 1.4×10^{-3} . Three graphite wafers were placed on the top of the gallium in the first experiment using this furnace, the aim being to coat these with GaN for subsequent regrowth in a stirred, vertical crucible.

The gallium was observed to move about 1 inch from the hot end on raising the temperature to the steady value, so that one wafer fell to the bottom of the crucible. Nucleation of GaN began around the edge of the wafer at the colder end of the crucible, and the nucleation of small crystals subsequently occurred around the end of the liquid. Further nucleation was observed on the liquid surface ahead of the established nuclei, so that a discontinuous GaN film spread from the cold end and, to a lesser extent, from the walls. After a week, nucleation could also be detected on the central graphite wafer. Only after about 10 days did the crystals nucleated at the cool end begin to grow appreciably larger. The largest crystals grew at the hot end, around the graphite wafer and the edge of the melt.

2. Compartmented Boat Technique

Experiments using a vertical crucible had indicated that transport of GaN in Ga is very sluggish by convection or diffusion, and this was confirmed by an experiment in a horizontal boat in which only a small area was exposed to the ammonia flow. Since the GaN appeared to form primarily by a surface reaction between the gallium and the ammonia, it was decided to adopt a compartmented boat arrangement in which the vitreous carbon boat was replaced by a silica tube indented at regular intervals by several mm to make 5-10 separate compartments (Fig. 2). The compartmented crucible was again located in a temperature gradient, with temperatures of 1010°C and 825°C at the ends of the compartmented section. The ratio of ammonia to hydrogen flows was initially 2×10^{-3} , as in the experiments of Logan and Thurmond, and the hydrogen flow rate was about 200 cm³/min. The direction of gas flow was from the hot end to the colder, and the reaction proceeded for 12 days in each case. Prior to crystal growth, the furnace was purged with hydrogen for 21 hours at room temperature, followed by 24 hours at about 1200°C.

In the first experiment, each compartment contained a drop of gallium weighing about 1.5 g. The aim of this experiment was to study the relative importance of surface and bulk reactions and to investigate the temperature dependence of the GaN formation reaction in the absence of convective flow along a continuous gallium sample.

It was found that at the hotter end of the crucible, the gallium drops had reacted almost completely to form GaN. The remaining gallium was in the form of fine inclusions trapped between GaN crystals. The resulting polycrystalline GaN product was in the form of a hollow dome, with rather larger crystals on the inside of the dome than on the outside. The initial reaction occurs at the Ga surface but this result is evidence of short-range transport of dissolved GaN to the interior of the sample as the reaction proceeds. At temperatures just below 1000°C, the GaN did not form a crust to prevent further reactions but sufficient space between crystallites remained to allow the reaction to continue almost to completion over a period of several days.

At lower temperatures the GaN formation reaction was incomplete, and a relatively thin crust was formed during the period of the experiment. Simultaneously with the reaction to form GaN, there was loss of gallium which was strongly dependent on temperature. The sample at the hottest end was almost completely lost by evaporation or by reaction with an impurity (e.g., oxygen) in the gas stream. The evaporated gallium reacted with ammonia and was deposited as a coating inside the silica liner in the region at temperatures below about 900°C. The hydrogen used in these experiments was normal commercial grade, and $\beta\text{-Ga}_2\text{O}_3$ was sometimes detected as deposits on the walls of the silica tube.

GaN whiskers were observed on samples which were at temperatures below about 950°C. The best crystals were formed by reaction at about 970°C and 990°C, where crystals 0.6 to 1 mm in size were grown, the best-developed faces being at the edge of the gallium where it contacted the silica crucible. Even in the best samples, however, there was multiple nucleation and the larger crystals grew in competition with many smaller crystals.

This experiment demonstrated that similar crystals could be obtained without a temperature gradient along a long sample of gallium (as in the Logan and Thurmond experiment). Although surface reaction between Ga and NH_3 was clearly dominant, there was evidence of bulk flow of dissolved GaN to deposit material inside the Ga drops. A temperature of about 980°C appeared optimum for crystal growth.

In the second experiment, polycrystalline seeds typically 4 mg in weight were inserted in each of the compartments, and the gallium contained in a silica boat located remotely at the hot end of the furnace. The same flow of $\text{NH}_3 + \text{H}_2$ was maintained over the gallium, the aim being to determine whether vapor transport either by reaction with gallium vapor, or via oxygen impurities in the hydrogen, would give growth on the seeds. Vapor transport was found in several experiments to produce coatings of GaN on the silica liner of the furnace.

SEM photographs of the seeds after this experiment showed no detectable GaN growth. However, some crystals were covered with very

fine needles of $\beta\text{-Ga}_2\text{O}_3$, as a result of an air leak which occurred over the last two days of the experiment. The main conclusion was, however, that this type of arrangement is not promising for growing large crystals on seeds.

In the third experiment, Ga drops and polycrystalline seeds (with 5-10 crystals) were inserted together into the recesses in the same quartz crucible, and the experiment repeated. As in the first experiment, there was a net loss of weight of the first four samples (approximately 1010°C - 950°C) while samples in the cooler region all showed a weight gain. The first two samples ($T > 990^\circ\text{C}$) showed evidence of decomposition, presumably through the reaction



The best-formed crystals were those grown in the range from about 970°C to 880°C ; again the largest crystals grown were about 1 mm in largest dimension. Although in most cases the larger crystals were self-nucleated and grew in competition with the seeds, sample #2 (approximately 850°C) apparently grew by the addition of growth hillocks, presumably at sites where screw dislocations intersected the surface (Fig. 3). The growth rate at this temperature was low, the crystal increasing in weight from 5.1 mg to 6.4 mg over 10 days. This example demonstrates that secondary nucleation can be avoided but the morphology of the grown layer is not smooth at this temperature. The density of active dislocations is in the region of 10^4 cm^{-2} . This crystal was the only example in this investigation where it was found possible to achieve growth on a seed without further nucleation.

Figure 4 is an example from the same experiment of a $\{0001\}$ surface of good morphology, free from hillocks or secondary crystals.

It was suspected that the purity and possibly the nucleation of the GaN crystals were influenced by traces of oxygen in the hydrogen, particularly since the color of crystals grown by chemical vapor transport was found to be strongly dependent upon the purity of the hydrogen carrier gas (39). For the final phase of this study, it was therefore decided to purify the hydrogen to reduce the oxygen concentration below 1 ppm. Initially a Matheson platinum catalytic purifier followed by

a liquid nitrogen trap was used, but it was found difficult with this arrangement to achieve substantial improvement in the H₂ purity.

A palladium diffusion furnace was therefore borrowed from another project and the gas flow system rebuilt using only high quality components also borrowed from the same project. This system was carefully checked for leaks and the moisture content of hydrogen leaving the system was determined by dew point measurement. The ammonia flow rate was controlled by a high quality needle valve since attempts to locate a massflow controller to deliver ammonia at rates below 10 cc/hour were not successful. The ammonia flow rate was monitored on a daily basis by dissolving the residual gas in water and titrating against 1N NCl.

After constructing and testing this system it was found that the diffusion furnace was ineffective, the dew point of hydrogen into and leaving the furnace having the same value (-46°C), although the palladium membrane was vacuum-tight. The experiments were therefore performed using pre-purified hydrogen. The dew point of this gas was below the limit of detection of our thermocouple, -80°C. In view of the cost of high purity hydrogen, the flow of carrier gas was reduced in the final series of experiments from 200 to 100 cc/min., this value remaining stable to within $\pm 10\%$ during the course of the experiment provided that occasional manual adjustment was made to the pressure regulator or needle valve.

Four experiments of 10 day duration were performed with the ammonia to hydrogen ratio varied from $(0.34 \pm 0.06) \times 10^{-3}$ to $(2.26 \pm 0.32) \times 10^{-3}$. The errors quoted are standard deviations, normally based on daily measurements of the ammonia flow by titration of the dissolved effluent. The ammonia pressures are, of course, reduced by the reaction with the gallium and the values quoted are those based on the ammonia concentration in the effluent stream. The actual ammonia partial pressure at the input (hotter) end of the furnace was higher, under conditions where the reaction was occurring and the ammonia concentration reduced downstream. GaN seed crystals were placed in the second and fourth compartment, the others containing only gallium weighing about 0.7 g, except for the experiment at 1.08×10^{-3} partial pressure when an α -SiC seed was introduced with the gallium.

The results of these experiments are summarized in Table 5 in the form of two parameters: the mass of GaN produced in a particular compartment, and the length of the largest crystal grown. The temperatures quoted are the average (to within 1°C) of each compartment, the difference in temperature across each sample due to the temperature gradient being about 20°C. These temperatures remained stable during the course of an experiment to better than 1°C.

It may be seen from Table 5 that no GaN could be detected when the partial pressure of ammonia was below 0.34×10^{-3} . When the partial pressure was raised to 0.69×10^{-3} , no nucleation occurred on the unseeded gallium samples except at the highest temperature ($\sim 990^\circ\text{C}$) where 10 mg of powdery material formed as islands of tiny crystallites on the gallium surface (Fig. 5). Thurmond and Logan (20) quote an average estimate of the ammonia partial pressure over GaN of $\sim 1.0 \times 10^{-3}$ at 1000°C and $\sim 0.55 \times 10^{-3}$ at 900°C so our data are consistent with these estimates at least to the order of magnitude.

It is significant that growth occurred on seed crystals at 0.69×10^{-3} partial pressure at 900° and 960°C , more growth being observed at the lower temperature. Presumably there was competition between faster kinetics at the higher temperature and a greater supersaturation at the lower, where the equilibrium value of p is lower. In this experiment the supersaturation was the dominant factor but the reverse was sometimes seen. An increase of the partial pressure to 1.08×10^{-3} led to the nucleation of GaN crystals at all temperatures in the range studied as may be seen from the graphical data of Fig. 6. The SiC seed appeared to be a good substrate for GaN growth, since oriented crystallites formed along its edges and, to some extent, in the center of the faces. Unfortunately, it was not possible to determine the weight of GaN formed in each compartment when the partial pressure was raised to 2.3×10^{-3} because of the creeping film effect, which caused the gallium to migrate into adjacent compartments. As expected, however, the yield of GaN was higher at the higher ammonia concentration.

The largest crystal grown in this investigation was 2.5 mm long and 1 mm in diameter and grew on the SiC seed at an NH_3 partial pressure

Table 5. Summary of Data on Crystal Growth by Compartmented Boat Method

A. Crystal Size

<u>Experiment code</u>	<u>NH₃ partial pressure(x10³)</u>	<u>Crystal Size (mm) at Mean Temperature of:</u>				
		<u>870°</u>	<u>900°</u>	<u>930°</u>	<u>960°</u>	<u>990°</u>
D8	0.34 ± 0.06	0	0	0	0	0
D10	0.69 ± 0.07	0	0.6	0	1.0	0.025
D9	1.08 ± 0.11	1.1	1.4	2.5	0.9	0.1
D7	2.26 ± 0.32	0.7	0.7	0.5	0.5	0.6

B. Mass of GaN Formed

<u>Experiment code</u>	<u>NH₃ partial pressure(x10³)</u>	<u>Mass(g) formed in 10 days at Mean Temperature of:</u>				
		<u>870°</u>	<u>900°</u>	<u>930°</u>	<u>960°</u>	<u>990°</u>
D8	0.34 ± 0.06	0	0	0	0	0
D10	0.67 ± 0.07	0	0.242	0	0.065	0.010
D9	1.08 ± 0.11	0.216	0.780	0.823	0.191	0.490

of 1.08×10^{-3} at 930°C (Fig. 7). This pressure appeared to be about optimum for crystal growth as may be seen from Fig. 8, although more data points would be required for more precise establishments of optimum conditions. Crystals roughly 1 mm long grew in 10 days at temperatures between 870°C and 960°C , both by spontaneous nucleation and secondary nucleation on GaN seeds. At 990°C no crystals could be seen on the surface of the gallium drop but a substantial quantity of tiny crystals ($\sim 25 \mu\text{m}$) formed on the bottom surface of the gallium. This observation contrasts with the normal tendency of crystals to grow at or near to the surface of the Ga.

The use of a partial pressure of 2.3×10^{-3} resulted in crystals up to 0.6 ± 0.1 mm long as may be seen from Fig. 8. The crystal size data is presented in alternative form in Fig. 9 as isotherms of crystal size versus ammonia partial pressure. These plots indicate the approximate critical partial pressure for nucleation and growth on seed crystals.

The most disappointing feature of our results is that, although we determined approximate partial pressure limits for growth and nucleation of GaN, the use of a partial pressure below that required for primary nucleation led not to stable growth of seed crystals but to secondary nucleation on these seeds. This is illustrated in Fig. 10 which shows the clusters of rather small crystals which nucleated on the seeds at 900°C and 960°C and 0.69×10^{-3} partial pressure.

The habit of the GaN crystals was normally the simple hexagonal form with $\{1100\}$ and $\{0001\}$ faces predominating. Occasionally the end face was capped over as in the example of Fig. 11. The growth mechanism is of interest since crystals were observed to grow either below the gallium surface or projecting from the surface. When crystals were grown just projecting from the Ga surface and at fairly high ammonia partial pressure ($\sim 2.0 \times 10^{-3}$), growth hillocks could be seen especially on the $\{0001\}$ faces. Hillocks can be seen in Fig. 1 and also in the example of Fig. 12. This type of hillock growth is commonly seen in crystals grown from high temperature solutions, very similar hillocks being seen, for example, on flux-grown GdAlO_3 (46) or on silver crystals

grown by electrodeposition (47). In the latter case, the hillock centers could be readily identified as points where screw dislocations emerged on the crystal surface. Crystal growth by a layer mechanism is more frequently observed on GaN and examples of both {0001} and {1100} faces are shown in Figs. 13-14. The layer sources are more probably the edges of a crystal face rather than defects near the face centers.

Hollow crystals are not uncommon, several examples being visible in the cluster shown in Fig. 15(a). In these examples, the {1100} faces are complete but the {0001} are absent. A magnified view of a hollow crystal is shown in Fig. 15(b).

We believe that the hollow crystals may be formed by a unique instability mechanism. If the crystal is growing out of the gallium melt into the surrounding vapor, the gallium which is needed for GaN growth probably arrives at the tip of the crystal by the creeping effect associated with its strong wetting action with GaN. The {1100} faces are therefore adequately supplied with gallium and are relatively well formed, as is confirmed by the SEM photographs. The {0001} end face grows by a mechanism of spreading from the edges of the face as Ga reacts with NH_3 , the growth rate being determined by the rate of transport of Ga. Small crystals have well formed end faces but, as the crystal grows, the flow of Ga by creeping may not be sufficient to supply the whole of the {0001} face. A depression therefore develops as shown in Fig. 16(a), which also shows a ridge around the edge of the face. As the crystal grows, the depression at the face center becomes deeper and subsidiary depressions may develop, as shown by the example of Fig. 16(b). Further growth leads to extension of the {1100} "walls," but gallium fails to reach the central region of the end face, so the hollow crystals of Fig. 15 result. Hollow crystals were not seen when growth took place below the gallium surface.

The color of crystals grown with purified hydrogen is amber, and the crystals are transparent as illustrated by the example of Fig. 17. This crystal shows banding and strain not normally associated with crystals grown from solution at relatively slow rates. The main impurity in the crystals is silicon which enters the material either

by direct reaction between Ga and the SiO_2 crucible or, more probably, via the gas phase due to the reaction between hydrogen and silica. In subsequent studies it is desirable to replace silica by alumina or carbon.

The conductivity along the c-axis of crystals grown using purified hydrogen is $(100 \pm 50) (\text{ohm cm})^{-1}$. This is of the order of magnitude expected for $n_e \sim 10^{19} \text{ cm}^{-3}$ and $\mu \sim 10^2 \text{ cm}^2 \text{ V}^{-1} \text{ s}^{-1}$, which are typical values for material prepared by the $\text{GaCl} + \text{NH}_3$ chemical vapor transport method (see Table 1). It has not been established whether the high conductivity is due to native donors or to impurities, but the former appears likely. The major impurity detected in our material is silicon, a shallow acceptor, and this could be reduced in concentration by using a silica-free system.

C. Vertical Crucible

The use of temperature gradient transport of GaN in a vertical crucible was considered at the start of this investigation to be one of the most promising for the growth of large crystals. This has been a successful technique for crystal growth of other sparingly soluble materials, and the minimization of surface area is normally beneficial since nucleation at the surface of the solution may then be more easily avoided. The supersaturation is normally controlled by changing the temperature difference between nutrient material and a seed crystal, and a large ΔT can be used to compensate for a low solubility.

In the first series of experiments, the temperature gradient was opposed to gravity so that slow transport of solute would occur only by diffusion possibly aided by solutal convection. This arrangement was found to be ineffective and complete dissolution of the seed crystal located at the cooler lower end of the crucible normally occurred. The gradient was therefore reversed in order to promote convective flow of solute from the GaN source material held at the crucible base to the upper region where a polycrystalline GaN seed was located. A temperature difference of 20-30°C was maintained across a 3 1/2" column of gallium, with a flowing NH_3/H_2 ambient above the gas. The ammonia partial

pressure was maintained close to the equilibrium value of 1×10^{-3} . After 16 days, it was found that the source material had gained weight but the seed dissolved. A similar result was obtained when the temperature difference was increased to 80°C.

It was therefore postulated that GaN has a reciprocal solubility in Ga, at least over the temperature range around 900°C. In order to confirm this hypothesis and to attempt to achieve crystal growth in either the hotter or cooler region of the vertical crucible, the apparatus was rebuilt to allow the stirring of the liquid by a 2-paddle arrangement. Two graphite paddles $3/4'' \times 1/2'' \times 1/8''$ were held centrally on a graphite rod, one being located near to the bottom of the melt while the other was $3 \ 1/4''$ higher on the rod. This rod was located axially in a $1 \ 1/4''$ diameter graphite crucible which was filled with gallium to a level about $1/2''$ above the upper paddle.

Prior to mounting, the paddles were coated with GaN by floating them on the surface of gallium in a vitreous carbon crucible. The crucible was maintained in a temperature gradient between limits of 920°C and 960°C and an ammonia/hydrogen mixture with partial pressure of 0.6×10^{-3} was passed over the gallium surface. GaN crystals grew in clusters on the paddles, the mass deposited in 10 days being 0.145 and 0.175 g, respectively.

The vertical crucible was heated to 1000°C at the lower paddle location and 960°C at the upper paddle location, and the shaft was rotated at 10 rpm. A gas stream of NH_3 (0.2 cc/min) and Ar (650 cc/min) was passed over the crucible. After 11 days the experiment was terminated and the paddles weighed. To our surprise, instead of one paddle losing weight and the other gaining weight, they both decreased in weight. The top paddle, which had 0.175 gm GaN, lost 0.065 gm, while the bottom paddle lost 0.026 gm. This result suggests that the liquid phase was undersaturated with respect to nitrogen in spite of the NH_3 content in the gas phase. This implies that the NH_3 did not decompose to produce its equilibrium partial pressures of N_2 and H_2 . The greater loss in weight at the lower temperature is consistent with a reciprocal solubility.

D. Crystal Growth from Ga/Sn Alloys

It was reported earlier that Ga/Bi alloys were generally found to result in more copious nucleation than Ga alone. A literature survey was undertaken to identify an alternative alloying element that might give superior results to pure gallium, and tin was chosen as the most promising candidate. The Ga/Sn phase diagram is a simple eutectic with no compound formation, and the melting points of both elements are conveniently low. The major advantage of tin, however, is that Parlee and co-workers have shown (43) that it reacts with nitrogen gas to give atomic nitrogen in solution. The attractiveness of tin is therefore that it should increase the concentration of dissolved atomic nitrogen in Ga/Sn alloys compared with the very low values characteristic of pure gallium.

In order to test this hypothesis, the compartmented boat technique was used with pure Ga replaced by Ga/Sn alloys with the concentration varying from 90Ga/10Sn to 20Ga/80Sn in 10 compartments. Nitrogen gas was used in place of the NH_3/H_2 mixture, with a slow flow rate of ~ 150 cc/day. It was noticed that the solutions migrated from the hot end to the center compartments (#'s 4-6). Some GaN growth was observed although a significant quantity of oxide was also formed ($\beta\text{-Ga}_2\text{O}_3$ plus various Sn oxides), especially at the cold end. The oxygen was presumably an impurity in the nitrogen.

The next attempt involved the use of GaN seeds in Ga/Sn alloys with a controlled NH_3 flow and purified H_2 . Compartments containing Ga and Ga/Sn alloys alone were alternated with seeded compartments in a 6-section boat. The results were disappointing--no additional growth of GaN seeds occurred in either Ga + Sn alloys or Ga alone. The material formed was small-grained polycrystalline GaN and all the crystals were black.

A further experiment was performed using a 5-compartment boat and a gas mixture of N_2 (400 cc/min) plus NH_3 (0.2 cc/min). The compositions ranged from 90% Ga - 10% Sn to 20% Ga - 80% Sn and the temperature from 970°C to 920°C. A great deal of vapor reaction was observed and the two compartments at the cold end were almost empty after a

12-day run while a fine white powder (presumably GaN) was exhausted through the furnace outlet. The solvent in the other three compartments had run together producing a silvery colored sponge material with no GaN crystals of any significant size. In a final experiment where the Sn and Ga were separated, powdery GaN was formed on the walls of the silica tube and there was creeping of the gallium over this powder, but no GaN crystals formed in the melt.

E. Summary of Main Conclusions

- (1) It has been confirmed that the solubility of GaN in gallium in the range from $\sim 850^{\circ}\text{C}$ to 1000°C is very low, probably $\sim 10^{-5}$ g GaN/g Ga; the solubility appears to have a retrograde dependence on temperature.
- (2) Above 750°C , gallium wets GaN very strongly and the creeping film effect increases with temperature and with increasing ammonia partial pressure.
- (3) Argon gas replacing hydrogen at the same flow rate leads to more rapid growth of smaller crystals.
- (4) Copious nucleation occurs over a range of temperatures and pressures and is difficult to control.
- (5) An ammonia partial pressure of above 0.36×10^{-3} is required for GaN nucleation; 0.7×10^{-3} leads to growth on seed crystals but by secondary nucleation.
- (6) The optimum temperature for crystal growth is in the range from 900°C to 970°C . At $\sim 1000^{\circ}\text{C}$ the rate of decomposition is appreciable and only small crystals form; below about 900°C crystals of nm size may grow but the yield is low.
- (7) Convective flow of atomic nitrogen is very sluggish even with a large thermal driving force.
- (8) Ga/Bi alloys were found to increase the nucleation frequency, in contrast to the results of Logan and Thurmond (19), but this result may be influenced by the fact that purified hydrogen was not used in this phase of our investigation.

- (9) GaN can be synthesized by the reaction between nitrogen gas and Ga/Sn alloys, but the crystals are very small.
- (10) Temperature gradient-driven flow of dissolved nitrogen is not a significant factor in crystal growth of GaN by this method. The most important method of crystal growth is by a vapor-liquid-solid (VLS) mechanism involving a creeping film of gallium. An instability mechanism characteristic of this unusual mechanism has been tentatively identified.
- (11) Some of the experimental results lead one to suspect that the ammonia decomposition reaction is being catalyzed by special metallic constituents in the reaction chamber and that kinetic rather than thermodynamic factors are controlling. Thus, the local environment conditions with respect to gaseous species and concentrations may vary somewhat from experiment to experiment even when the far-field parameters of gas composition, flow rate, temperature, etc., are held constant.
- (12) The large bandgap of GaN favors the development of a strong interface field wherein the monatomic nitrogen species forms. The electrical effects due to band bending and space charge screening are thought to prohibit the effective growth of large GaN crystals.
- (13) The theoretical ideas proposed here should apply to vapor growth of GaN as well as to solution growth.
- (14) We do not recommend any practical crystal growth on this system without first conducting the proposed basic studies (page 36, section A).
- (15) The theoretical ideas proposed here for GaN should be applicable to all large bandgap semiconductors.

IV. THEORETICAL MODEL

The key experimental observation that leads us to a theoretical toehold on a model that may rationalize the majority of the observations is the "creeping effect." This is a special wetting phenomenon which indicates that the interfacial energy between Ga and GaN, $\gamma_{\text{Ga/GaN}}$, is very small. Creeping only occurs after a film of GaN forms on the boat immediately adjacent to the Ga melt (19). To understand why this is so, one needs to consider the electronic contribution to the interfacial energy, γ_e (44). We shall see that the interface electrostatic potential, ϕ_s , becomes an important consideration in that it determines the magnitude of the interface field penetrating into the Ga melt. This interface field is thought to strongly dissociate the dissolved N_2 into 2N which behaves like an electrolyte in the interface region. Because of this, small crystals can be thought to act on each other much like colloidal particles. Let us look at the various pieces of the puzzle in turn.

A. Free Electron Term γ_e

The interfacial energy $\gamma_{\text{Ga/GaN}}$ can be written as

$$\gamma = \gamma_0 + \gamma_e \quad (1)$$

where γ_e is the free electron contribution and γ_0 is the sum of the non free-electron contributions. The Lippman equation (44) developed almost a century ago for ion distributions tells us that

$$\gamma_e = -\int_0^{\Delta\phi} \sigma d\phi \quad (2)$$

where σ is the charge density in any slice parallel to the interface and $\Delta\phi$ is the total Galvanic potential difference across the space charge layers at the interface. The space charge layers come about because of the difference in Fermi energy, E_F , for the electrons.

When ΔE_F is large, many electrons will spill over from the higher E_F phase to the lower between the GaN and the Ga. From eq. (2), we find that γ_e is always negative and large in magnitude when two conductors are in contact and when a large value of $\Delta\phi$ exists between them. Using a simple two-layer capacitor model, the charge density σ is given by

$$\sigma = \frac{\pi}{4} \left(\frac{1}{\frac{d_1}{\epsilon_1} + \frac{d_2}{\epsilon_2}} \right) \Delta\phi, \quad \begin{array}{l} 1 \equiv \text{Ga} \\ 2 \equiv \text{GaN} \end{array} \quad (3)$$

where $\tilde{\epsilon}$ refers to the permittivity of the phase and d refers to the Debye length for the space charge in the phase; i.e.,

$$d = (\epsilon kT / \epsilon \pi e^2 n_\infty)^{1/2} \quad (4)$$

where e is the electronic charge and n_∞ is the electrolyte concentration in the bulk of the phase.

When a conductor is in contact with a thick nonconductor, the magnitude of $-\gamma_e$ is relatively small because most of the space charge is developed in the nonconductor (σ is small because $d_2/\epsilon_2 \gg d_1/\epsilon_1$ in eq. (3)). However, when the nonconductor is very thin (less than the Debye-length for the material), the space charge must develop in the conductor and this greatly increases $|\gamma_e|$. Thus, as a nonconductive film thickens, its interfacial energy, γ , increases and its interfacial potential, ϕ_s , changes (from a high to a low value or vice versa depending upon the relative E_F values for GaN and Ga).

B. Interface Electrostatic Potential ϕ_s

The interface electrostatic potential, ϕ_s , relative to the bulk value, $\phi_{\infty 1}$, in the Ga depends on the electron affinity, χ , and the work function, W , of the two materials. Let us suppose that the values of χ and W for Ga and GaN are such that $E_{F2} > E_{F1}$ so that electrons are transferred from phase 2 (GaN) to phase 1 (Ga) to bring about electronic equilibrium. The Ga is a poor metal but is still a fair conductor compared to GaN at approximately 800°C. Thus, the potential distribution across the interface for a thick and a thin GaN film may be represented as in Fig. 18. Fig. 19 provides a qualitative variation of ϕ_s with GaN film thickness, λ . We see that ϕ_s decreases from a maximum value to a minimum value as λ increases to values such that $\lambda \gg d_2$. From eq. (3) with an interface charge density ρ_1^* and Gauss' law, we have

$$\phi_s - \phi_{s1} = \frac{(\epsilon_2/d_2)\Delta\phi - \rho_I^*}{(\epsilon_1/d_1 + \epsilon_2/d_2)} \quad (5)$$

The value of ϕ_s will also change with the magnitude of E_{F2} which can be changed by doping of the GaN so that the conduction is extrinsic rather than intrinsic at the growth temperature ($\Delta\phi \propto E_{F2} - E_{F1}$). In addition, ϕ_s may change due to E_{F1} changes by alloying of the Ga. In pure GaN, we expect the free electrons to come from two possible sources, (a) band-to-band transitions and (b) the formation of nitrogen or gallium vacancies to act as donors or acceptors respectively. If electrons come from the ionization of a nitrogen vacancy, the relationship between the electron concentration and the ammonia pressure can be calculated from



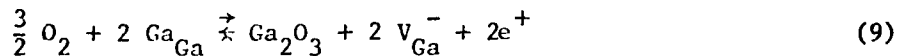
and

$$\frac{P_{NH_3}}{(P_{H_2})^{3/2}} [V_N^+] [e^-] = K_1 \quad (7)$$

If the electron and vacancy concentrations are equal

$$[e^-] = K_1^{1/2} P_{H_2}^{3/4} P_{NH_3}^{-1/2} \quad (8)$$

Analogue equations can be obtained for the Ga vacancy acceptors if oxygen is present in the system; i.e.,



and

$$\frac{[Ga_2O_3] [V_{Ga}^-] [e^+]^2}{P_{O_2}^{3/2}} = K_2 \quad (10)$$

Thus, the presence of a small amount of oxygen in the system (perhaps from wet H_2) is expected to reduce $[e^-]$ in eq. (8), to reduce the Fermi

energy of the GaN somewhat and thus to decrease the Galvani potential difference, $\Delta\phi'$, between the Ga and the GaN. We expect $\Delta\phi$ and thus ϕ_s to increase as the reaction expressed by eq. (6) is driven to the right.

To understand possible melt alloying effects, we consider the alterations in the thermodynamic activity of Ga in the reaction



and

$$\frac{\tilde{\gamma}_{\text{Ga}} X_{\text{Ga}} P_{\text{NH}_3}}{(P_{\text{H}_2})^{3/2}} = K_3 \quad (12)$$

where $\tilde{\gamma}_{\text{Ga}}$ is the activity coefficient of Ga in the solution. It is unlikely that this reaction will dominate the formation of Ga or NH_3 but, if it did, X_{Ga} would be inversely proportional to P_{NH_3} and from eq. (8) we would expect

$$[e^-] \propto X_{\text{Ga}}^{1/2}. \quad (13)$$

Thus, as X_{Ga} decreases, for fixed $\tilde{\gamma}_{\text{Ga}}$, $[e^-]$ will decrease which means that the extrinsic conduction decreases. The Fermi level will thus move back towards midband and ϕ_s will decrease for fixed γ as X_{Ga} decreases.

Since K_1 in eq. (7) varies as $\exp(-\Delta H^\circ/RT)$, as T is decreased, K_1 is expected to decrease and so will $[e^-]$. However, the intrinsic electron concentration will also decrease exponentially with T and, to see whether E_{F2} decreases or increases with T changes, we must compare the magnitude of ΔH° for the formation of the V_{N}^+ defect with the bandgap energy of GaN. We should also note that, at fixed T, as we substitute argon for H_2 as the carrier gas, $[e^-]$ will decrease from eq. (8) and so will E_{F2} if extrinsic conduction had been dominating in the H_2 carrier gas case. In this situation, ϕ_s is expected to decrease as the H_2 content decreases

C. Interface Field Effects

Let us postulate that monatomic nitrogen has a strong electron affinity and develops an associated negative charge in the liquid Ga. It will thus be attracted to the more positive electrostatic potential $\phi_s - \phi_{\infty 1}$ of the interface. The electrostatic potential distribution in the Ga will bind the N^- species with a free energy $\Delta G_1^\circ(x)$ given by

$$\Delta G_1^\circ(x) = \Delta G_1^\circ(0)e^{-\rho x} \quad (14)$$

where $\rho \sim d_1^{-1}$ and $\Delta G_1^\circ(0) < 0$. As a result of this, the equilibrium distribution of monatomic nitrogen species, $C_0^N(x)$, is given by

$$C_0^N(x) = C_{00}^N \exp(-\Delta G_1^\circ(x)/(kT)) \quad (15)$$

where C_{00}^N is the bulk value (see Fig. 20).

From the N_2 dissociation reaction in the Ga, we have



with

$$\frac{[\tilde{\gamma}_N X_N]^2}{[\tilde{\gamma}_{N_2} X_{N_2}]} = K_4 \quad (17)$$

so that

$$X_N(x) = \frac{\tilde{\gamma}_{N_2}^{1/2}}{\tilde{\gamma}_N} X_{N_2}^{1/2} K_4^{1/2} \exp(-\Delta G_1^\circ(x)/(kT)) \quad (18)$$

Thus, even though X_{N_2} is very small in the bulk Ga, X_N can be large in the interface region² provided $-\Delta G_1^\circ(0)/kT$ is large. This is expected to be the case if $\phi_s - \phi_{\infty 1}$ is large and positive. Such a situation would explain the strong surface activity of nitrogen in general and would predict that N could not be readily transported through bulk liquid Ga because it would recombine to form N_2 in the fluid volume outside of the interface field region. Because of the foregoing we may conclude that the formation of GaN via the reaction



is not thermodynamically limited. Rather, we expect it to be kinetically limited by the unavailability of N rather than N_2 . Only the reaction



is expected to be favorable for film formation.

If GaN crystals have a positive surface potential, ϕ_s , and monatomic N acts as if it has a negative charge, N^- , then a number of small GaN crystals may stay dispersed from each other or agglomerate into a close group depending on their colloid-like behavior. From colloid theory⁽⁴⁴⁾, we know that it is the van der Waals electrodynamic forces between particles that provide the attraction while the double-layer electrostatic forces provide the repulsion. The combination of these two forces gives rise to a resultant interparticle potential distribution as illustrated in Fig. 21. In our case the Debye length around a crystal is given by eq. (4) with n_∞ determined by C_{00}^{N} in eq. 15. Since we expect C_{00}^{N} to be extremely small, d_1 will be fairly large for these ions and the small crystals will stay dispersed. In this case, liquid gaps are maintained on the surface via which N_2 may enter the Ga solution and dissociate to yield the N needed to continue the GaN crystal growth. As the crystals grow thicker, ϕ_s decreases so that d_1 also decreases and crystal agglomeration tends to occur on the melt surface at some particular crystal size. As the temperature is lowered, d_1 is decreased via eq. (4) and since ϕ_s is probably also decreased, the crystals do not grow as large before the attractive forces for agglomeration dominate. Of course most of these agglomerated crystal masses will be bound in the secondary potential minimum of Fig. 21, so that surface gaps still exist to slowly feed the growing crystals. Below some critical temperature, the agglomeration forces set in and are of such magnitude that binding in the primary potential ($r < r_0$) occurs at crystal diameters less than 1 micron so that only a very thin and tenuous GaN film forms to cover the liquid surface. This inhibits the growth to larger film thicknesses because there are no surface liquid gaps through which N_2 can enter. From this we see that the effective solubility of GaN, as determined by crystal mass in an experiment, will strongly decrease with decrease of temperature.

D. Rationalization of Experimental Observations

(1) Creeping Fluid Effect: This is a clear manifestation of a strongly reduced $\gamma_{\text{GaN}}/\gamma_{\text{Ga}}$, probably due to a large negative value of γ_e . Since $|\gamma_e|$ should be larger for thin GaN films than for thick films, the wetting effect should be strongest for newly formed films.

(2) Copious Nucleation Rate: As $p_{\text{NH}_3}/p_{\text{NH}_3}^*$ (p^* is the equilibrium partial pressure) increases, the frequency of GaN crystal nucleation on the Ga surface increases very rapidly. Even for values of $p_{\text{NH}_3}/p_{\text{NH}_3}^* < 2$, a high nucleation frequency is observed. Such a situation requires an extremely low value of $\gamma_{\text{GaN}}/\gamma_{\text{Ga}}$ which is completely consistent with (a) above.

(3) Small Solubility and its Retrograde Nature: The true solubility of N or N_2 in liquid Ga per se has not been measured yet. What has been measured is the mass of GaN solid formed at a particular temperature per unit mass of liquid Ga available. This is generally small and it decreases with temperature.

The small value undoubtedly occurs because of the small bulk solubility of N_2 or N in liquid Ga but also because the film formation blocks the access of bulk liquid to the gaseous source. As the temperature is decreased, the colloidal-type coagulation of crystals quickly seals over the liquid-gas interface and negligible access exists for the gaseous source to communicate with the bulk liquid. Thus, an apparent retrograde type of solubility occurs. It is also possible that the apparent decrease in the dissolution rate of GaN in stirred, bulk Ga with increase of temperature is due to a genuine retrograde solubility. However, this effect could also be associated with kinetic effects at the GaN/Ga and Ga/vapor interfaces and this very limited evidence is inadequate to determine whether or not the apparent retrograde solubility is of thermodynamic origin.

(4) Temperature Effect: Since K_1 in eq. (7) decreases as T decreases, $[e^-]$ is expected to decrease so that the conduction disparity between GaN and Ga increases. This makes d_2 even larger so that the thin film effect on γ_e becomes even more important. The crystal coagulation phenomenon discussed above becomes the determining feature here.

(5) Apparent Lack of Convective Transport of N Atoms in Ga:

We found that, under temperature gradient conditions where strong convection should occur in the liquid, negligible transport of GaN or N occurred from a solid source to a sink. This is accounted for by eqs. (14-18) expressing the postulate that the formation of N from N_2 is enhanced only in the region of an interface field. Thus, if convective transport sweeps N out of the interface field region, it recombines fairly quickly to form N_2 and leaves the system so that N is not transported to the sink region to give controlled deposition.

(6) Alloy Addition Effect: As shown by eqs. (12) and (13), as X_{Ga} decreases, $[e^-]$ also decreases so that thinner films of GaN should form (for $\tilde{\gamma}_{Ga}$ ~ constant) and more polycrystallinity should result. This result is in agreement with our experimental observations but is in disagreement with those of Logan and Thurmond (19).

(7) Seeding Effect: We have generally found that adding GaN seed crystals to a Ga melt in the presence of a gaseous source does not enhance GaN formation on the seed crystal. This occurs because the growth kinetics of thick crystals are extremely slow since ϕ_s is greatly reduced leading to small values of nutrient N. In addition, copious nucleation of new crystals occurs on the surface. These are thinner and have larger ϕ_s so that the available N attaches at such surfaces rather than at the seed crystal surface. One would need to reduce the nucleation frequency to zero while still retaining a value of $p_{NH_3}/p_{NH_3}^* > 1$, in order to properly check out the seeding possibility. Very stable control of partial pressures would be necessary for careful studies of seeded growth and nucleation.

(8) Carrier Gas Effect: As we change from H_2 to Ar as a carrier gas, $[e^-]$ should decrease via eq. (7). Once again this will lead to a decreased ϕ_s for thick GaN so we should expect only a thin film of GaN to form in a fixed time so that a smaller mass yield of GaN should be observed. However, our comparisons were made at widely different partial pressures, the experiments in argon being at high p/p^* and therefore resulting in copious nucleation as discussed above.

(9) Catalysed Gas Reactions: The addition of Sn to the system, either as an alloying agent to Ga or as a separate small pure Sn melt

on the gas inlet side to the Ga, was found to greatly enhance the evaporative transport of Ga in the form of GaN so that only a slight amount of GaN formed on the melt and this was very fine grained. Logan and Thurmond(19) also found that the ageing of the silica tube in the reaction chamber influenced the NH_3 decomposition reaction. It seems that various metallic elements like Sn, Si, etc.. greatly influence the nature of the gas phase species.

V. EXPERIMENTS TO BE DONE

A. Fundamental Data

It appears that, before large crystals of GaN can be grown, an improved understanding of the factors which influence growth are necessary. Given a stronger data base, the particular problems limiting the growth of large GaN crystals should be capable of solution and we believe that cm size crystals could be grown given sufficient effort. Specific experiments are proposed as follows:

- (1) Using different carrier gases, alloying elements and furnace wall materials, mass spectrographic analysis should be made of the different species present in the gas as a function of temperature, alloying element, time, etc.
- (2) Using different substrates and the gas source from (1), the surface species should be determined by some appropriate technique.
- (3) Using different substrates with droplets of Ga, contact angle changes should be measured as a function of T and gas composition.
- (4) Using dry H_2 and mass flow meters, controlled supersaturation experiments, with precise mass flow controllers, should be made in the range $1 < p/p^* < 1.5$ to determine the nucleation frequency of GaN on Ga.

B. Alternative Methods of Preparing GaN

The study has identified a partial pressure region over which the growth of GaN by reaction between gallium metal and NH_3 in a hydrogen carrier gas is fairly well controlled. The use of this procedure using an optimum NH_3/H_2 flow ratio with intermittent replenishing of the gallium could be expected to give large crystals given sufficient time. If a crystal 1 mm long grows in ten days, then a period of about three months would be required to grow a 1 cm crystal.

The low solubility of GaN in Ga implies that it is unlikely that faster growth will be possible by a solution method. Since we have found that techniques which rely on bulk transport of atomic nitrogen in gallium are inappropriate, a method which uses the surface reaction between a thin film of liquid gallium and ammonia at a suitable partial pressure should be investigated. One method which suggests itself is to make drops

of Ga fall at suitable intervals onto a substrate or seed crystal and to rotate this seed at a sufficiently high rate for the film to adhere uniformly. The liquid film would be reacted fully before the next droplet landed.

This method suffers from the disadvantage that it is an intermittent process, so the film could suffer damage from the thermal shock caused by the arrival of a Ga drop at a lower temperature and it is difficult to devise an ideal method for delivering the drops. It would therefore be preferable to use an evaporative source to produce a steady flow of gallium to a substrate where it reacts with atomic nitrogen either from ammonia or activated N_2 . This approach is effectively that of molecular beam epitaxy and the growth of GaN by MBE should be investigated on a commercial apparatus. An alternative and more appropriate technique is the simpler version developed by K. Zanio and coworkers at Hughes Research Laboratories and called "planar reactive deposition." This method uses a heated source to generate a beam of metal atoms which is reacted with a gas stream on a heated substrate holder (45). It was used successfully to grow InP films by reacting PH_3 in a hydrogen flow with indium at substrate temperatures as low as $425^\circ C$. The reaction chamber is evacuated and contains a liquid nitrogen-cooled shroud to condense excess phosphorus.

Another alternative which should be pursued is conventional solution growth by slow cooling. The main problem is, of course, the choice of a suitable solvent. Nitride crystals have been grown from metal solutions but our experience with the most promising choices, bismuth, tin, and their alloys with gallium suggests that these are not appropriate for the slow-cool method because of the low solubility. Lithium nitride Li_3N with a melting point of about $845^\circ C$ appears to be the outstanding contender. It is stable, relatively easy to synthesize, and could be used to grow GaN in the range from about $1050-900^\circ C$ where it is fairly stable. The solubility is unknown but could be appreciable since the bonding is similar in the two materials. Studies of GaN/ Li_3N solutions would have been included in this program had more time been available.

C. Alternative Candidates to Replace GaN

It is quite clear from our two-year feasibility study that large GaN crystals will be difficult to prepare by solution growth techniques. However, during the last few months of the investigation, our systematic approach to the problem and the emphasis we placed on understanding the solidification behavior of GaN from Ga solutions started to yield important new data. We believe that more work of this type will result in better control of the solution growth process leading to improved crystal size and quality. If future programs on this subject are to be considered, it is recommended that funding be committed for a significantly greater time period than in this program so that the research effort can be carried out in a more efficient, professional manner. In any event, we believe a major commitment of both time and money will be required before large high quality GaN crystals can be produced by this method.

An alternative strategy for solving the immediate problem of developing good blue light emitting diodes is to look for other wide bandgap semiconductors. Prime candidates such as SiC and ZnS have not yet proved very successful, although apparently good quality SiC crystals have been reported by the group of Tairov and Tsvetkov in Leningrad and their approach looks worthy of further investigation. An exciting new possibility was recently suggested by Yamamoto (University of Osaka, Japan) at the International Conference on Ternary and Multinary Compounds, August 1980 in Tokyo. He considered the use of the ternary chalcopyrite compounds and their solid solutions for this application.

Only four of these compounds have a high enough bandgap to emit blue light: CuAlS_2 , CuAlSe_2 , AgAlS_2 , and AgGaS_2 . Of these, Yamamoto believed that CuAlS_2 was the best candidate since CuAlSe_2 and AgAlS_2 are unstable in air and AgGaS_2 has too high a resistivity. He proposed the use of a $\text{CuAl}_{1-x}\text{Ga}_x\text{S}_2/\text{ZnS}$ hetero-junction. In our opinion, this approach represents a viable new research area and we recommend that a program be initiated to study the synthesis, crystal growth, and properties of such wide bandgap materials. The chalcopyrites, while not the easiest class of compounds to

prepare in single crystal form, are much simpler than GaN. Stanford's Center for Materials Research has worked with compounds of this type for many years and has grown large high-quality single crystals of several of them, including AgGaS_2 and AgGaSe_2 .

VI. SUMMARY AND CONCLUSIONS

1. The largest crystals grown were 2.5 mm in length and 1 mm in diameter. These are the largest crystals reported by this technique, in terms of mass. Larger crystals could presumably be grown by the application of these growth conditions ($T \sim 930^\circ\text{C}$, ammonia partial pressure $\sim 1.0 \times 10^{-3}$) over long periods, with intermittent replenishing of the gallium.

2. It has been found that the minimum ammonia partial pressure (in hydrogen) for growth of GaN crystals in gallium solutions in the temperature range from 870°C to 990°C is above 0.34×10^{-3} molar.

3. As the partial pressure is increased to 0.7×10^{-3} , nucleation of GaN does not occur at 930°C or below, but nucleation of tiny crystals takes place at 999°C . At this partial pressure growth does occur on seed crystals.

4. Even at partial pressures where nucleation does not occur in the region away from a seed crystal, secondary nucleation occurs rather than growth of the seeds to a larger size.

5. Temperature gradient transport, in a horizontal or vertical crucible, was not effective in producing GaN crystals from Ga solutions. Growth occurs by a VLS mechanism, with gallium supplied to regions outside the liquid by flow in a thin film across the crystal surface.

6. GaN crystals appear to grow under a variety of experimental conditions by a layer mechanism, and an unusual form of instability was noted in which hollow crystals seem to form through inadequate supply of gallium by creeping along the crystal faces.

7. SiC appears a more satisfactory substrate material for growth of GaN than sapphire.

8. Bismuth alloying with gallium was found to increase nucleation. GaN was prepared by the reaction between nitrogen gas and Ga/Sn alloys but the particle size of material formed was very small.

9. A theoretical model which explains several of the observed phenomena is outlined. Many problems of growing GaN from Ga solution may be due to interface field effects associated with the growth of a wide band-gap material from a conducting solution.

10. Alternative methods for growing GaN bulk crystals which have not been investigated to date are proposed. In particular, methods involving the reaction between ammonia or activated nitrogen and a very thin film of gallium incident on a GaN seed appear to be particularly promising.

VII. REFERENCES

1. H. P. Maruska and J. Tietjen, Appl. Phys. Lett. 15, 327 (1969).
2. J. I. Pankove, J. E. Berkeyheiser, H. P. Maruska, and J. Wittke, Solid State Comm. 8, 1051 (1970).
3. D. L. Camphauser and G. A. N. Connell, Bull. Amer. Phys. Soc. 16, 305 (1971).
4. R. Dingle, D. D. Sell, S. E. Stokowski, P. J. Dean, and R. B. Zetterstrom, Phys. Rev. B, 3, 497 (1971).
5. R. Juza and H. Hahn, Z. Anorg. Allg. Chem. 239, 282 (1938).
6. D. Marchon, A. Barker, P. Dean, and R. Zetterstrom, Solid State Comm. 8, 1221 (1970).
7. B. B. Kosicki, R. J. Powell, and J. C. Burgiel, Phys. Rev. Lett., 24, 1421 (1970).
8. R. D. Cunningham, R. W. Brander, N. D. Knee, and D. K. Wickenden, J. Luminescence, 5, 21 (1972).
9. R. Dingle and M. Ilegems, Solid State Comm. 9, 175 (1971).
10. M. Ilegems and H. C. Montgomery, J. Phys. Chem. Solids, 34, 885, (1973).
11. J. I. Pankove, S. Bloom, and G. Harbeke, RCA Review, 36, 163 (1975).
12. J. I. Pankove, D. Richman, E. A. Miller, and J. E. Berkeyheiser, J. Luminescence, 4, 63 (1971).
13. R. Dingle, K. L. Shaklee, R. F. Lehem, and R. B. Zetterstrom, Appl. Phys. Lett, 19, 5 (1971).
14. J. I. Pankove, J. Luminescence 7, 114 (1973).
15. G. Jacob, Acta Electronica, 21, 159 (1978).
16. M. Lorenz and B. Binkowski, J. Electrochem. Soc., 109, 24 (1962).
17. M. Lyutaya and V. Bukhanevich, Russ. J. Inorg. Chem. 7, 593 (1962).
18. R. Groh, G. Gerey, L. Bartha, and J. I. Pankove, Phys. Stat. Sol. (9) 26, 353 (1974).
19. R. A. Logan and C. D. Thurmond, J. Electrochem. Soc. 119, 1727 (1972).

20. C. D. Thurmond and R. A. Logan, J. Electrochem. Soc. 119, 622 (1972).
21. W. Johnson, J. Parson, and M. Crew, J. Phys. Chem. 36, 2651 (1932).
22. R. C. Schoonmaker, A. Buhl, and J. Hemley, J. Phys. Chem. 69, 3455 (1965).
23. T. L. Chu, K. Ito, R. K. Smeltzer, and S. S. C. Chu, J. Electrochem. Soc. 121, 159 (1974).
24. M. Ilegems, J. Crystal Growth, 13/14, 360 (1972).
25. E. Butler, G. Fitzi, G. Leonhart, and W. Siefert, Thin Solid Films, 59, 25 (1979).
26. K. Gillesen, K. H. Schuller, and B. Struck, Mat. Res. Bull, 12, 955 (1977).
27. T. L. Chu, J. Electrochem. Soc. 118, 1200 (1971).
28. H. M. Manasevit, F. H. Erdmann, and W. I. Simpson, J. Electrochem. Soc. 118, 1864 (1971).
29. D. D. Manchon, A. S. Barker, P. J. Dean, and R. B. Zetterstrom, Solid State Comm. 8, 1227 (1970).
30. M. Aoki, M. Sano, and T. Ogino, Sago Shikense Nempo, 34, 125 (1975).
31. R. B. Zetterstrom, J. Mat. Sci., 5, 1102 (1970).
32. A. Addamiano, J. Electrochem. Soc. 108, 1072 (1962).
33. T. Ogino and M. Aoki, Oyo Butsuri, 48, 269 (1979).
34. B. J. I. Sherwood and D. K. Wickenden, J. Mat. Sci., 5, 869 (1970).
35. H. J. Hovel and J. J. Cuomo, Appl. Phys. Lett., 20, 71 (1972).
36. B. B. Kosicki and D. Kahng, J. Vac. Sci. Technol. 6 593 (1979).
37. J. C. Knight and R. A. Lujon, J. Appl. Phys. 49, 1291 (1978).
38. R. Madar, G. Jacob, J. Hallais, and R. Fruchart, J. Crystal Growth, 31, 197 (1975).
39. H. Kanber and M. Gershenzon, private communication.
40. I. G. Pichugin and D. A. Yaskov, Neorg. Mat. 6, 1973 (1970).
41. H. C. Grimmeis and G. Monemar, J. Appl. Phys. 41, 4054 (1970).
42. E. Ejder, J. Crystal Growth, 22, 44 (1974).

43. R. N. Anderson and N. A. D. Parlee, *Met. Trans.* 2, 1599 (1971) and private communication.
44. W. A. Tiller and T. Takahashi, *Acta Met.* 17, 483 (1969).
45. L. Fraas and K. Zanio, *J. Electronic Matls.* 7, 211 (1978).
46. H. J. Scheel and D. Elwell, *J. Crystal Growth*, 20, 267 (1973).
47. E. Budevski, R. Kaishev, V. Bostanov, and S. Toshev, Film "An Introduction to the Theory of Crystal Growth," (Bulgarian Academy of Sciences, 1966).

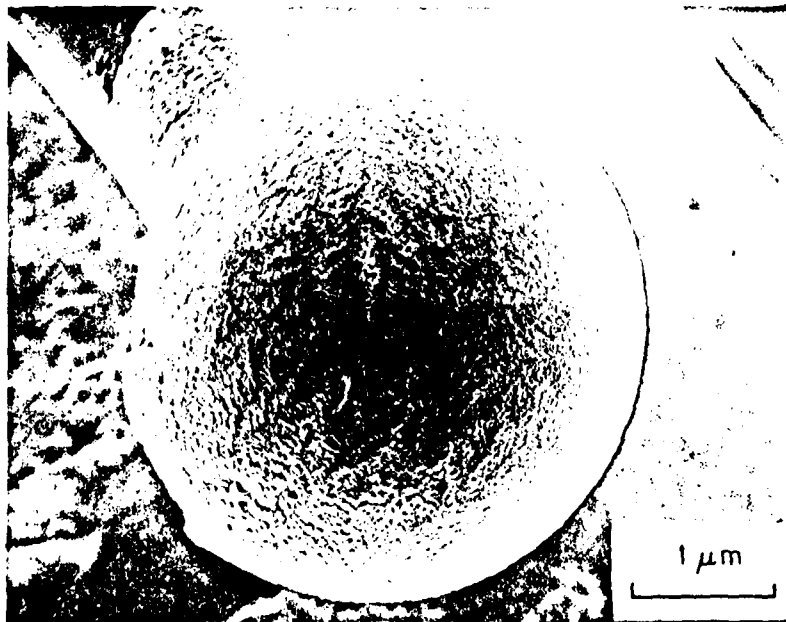
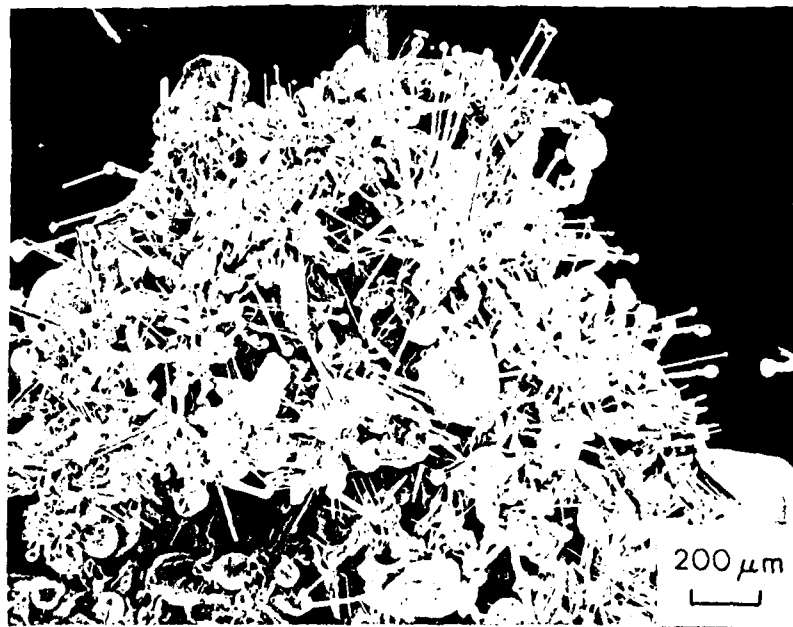


Fig. 1 (a) Cluster of GaN crystals apparently grown by conventional vapor-liquid-solid (VLS) mechanism, with gallium droplet on end of needle-shaped crystals (50 X).
(b) Close-up of Ga droplet on end of GaN needle (21,000 X).

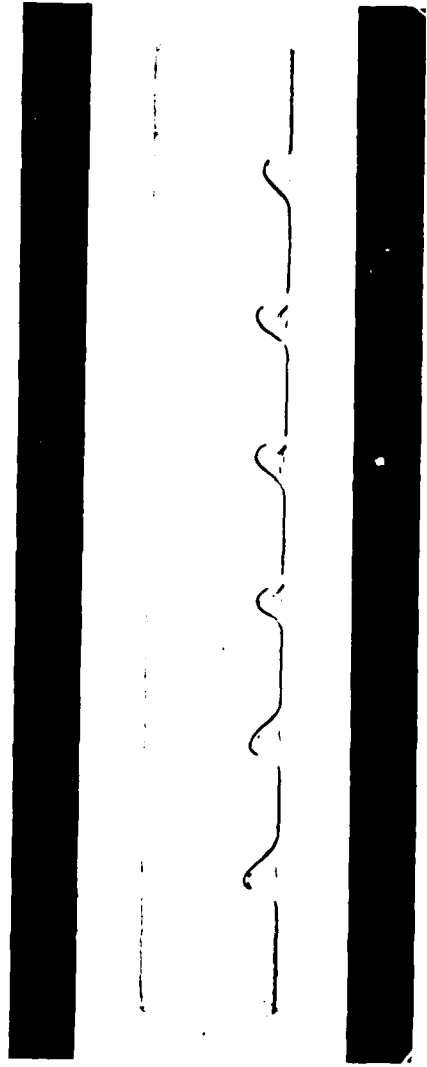
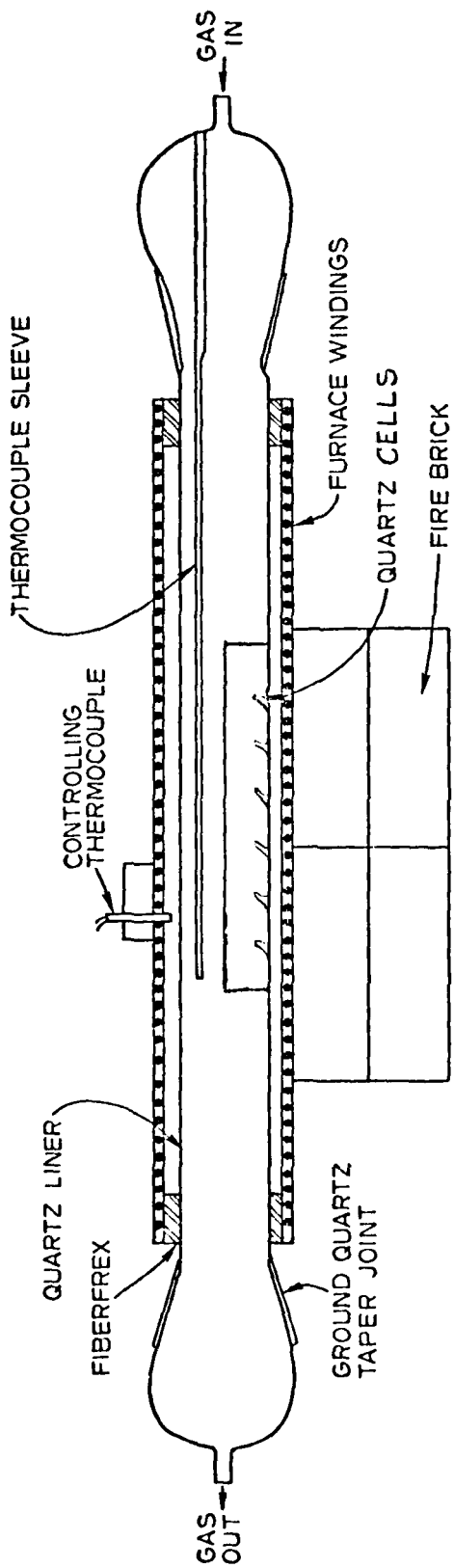


Fig. 2. (a) Apparatus used for growth of GaN in compartmented crucible (diagrammatic).
 (b) compartmented silica boat.

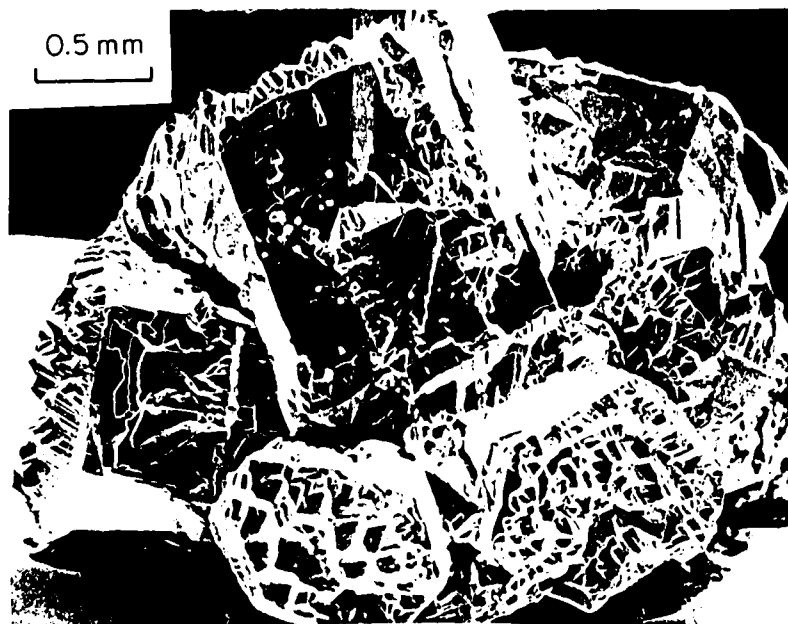


Fig. 3. Seed crystal showing additional growth by hillock mechanism (33 X).

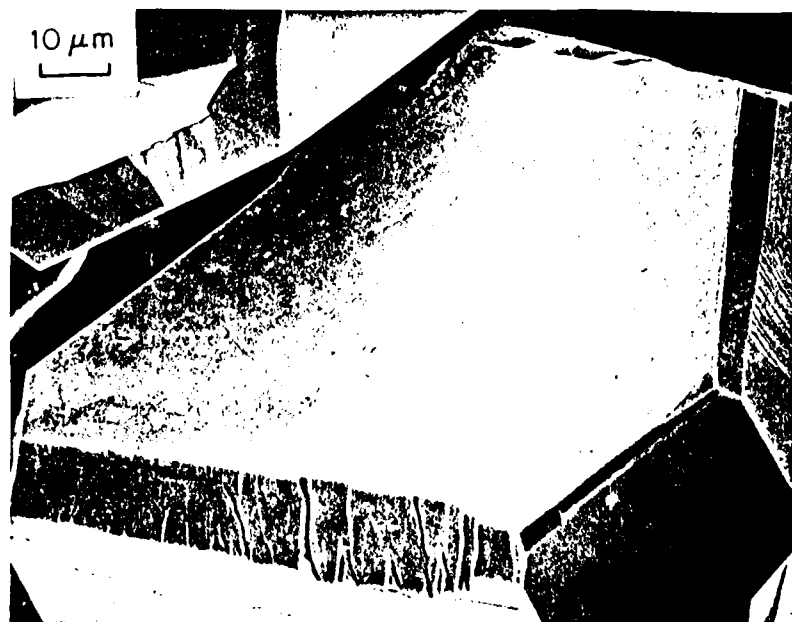


Fig. 4. {0001} face of GaN with no obvious growth features (1000 X).

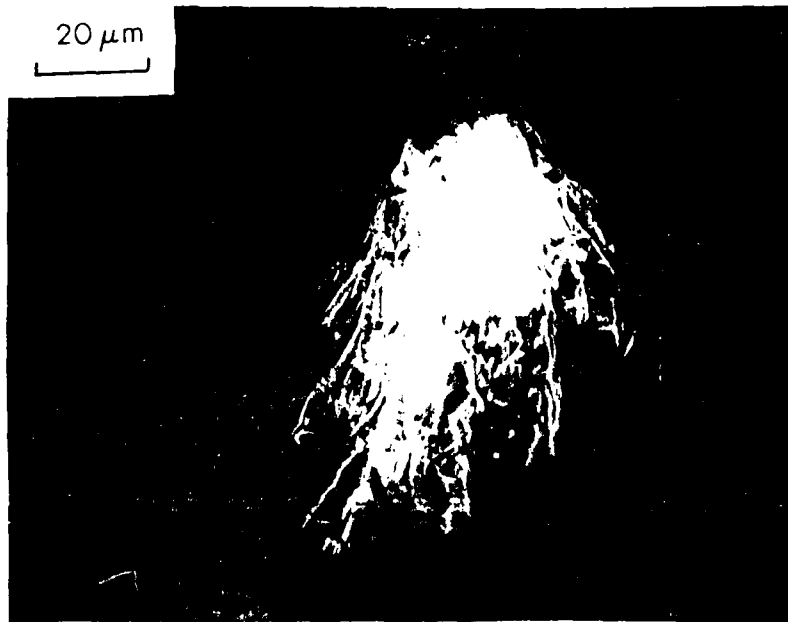


Fig. 5. Small crystallites of GaN nucleated as islands on the surface of Ga at 990°C and 0.7×10^{-3} partial pressure (800 X).

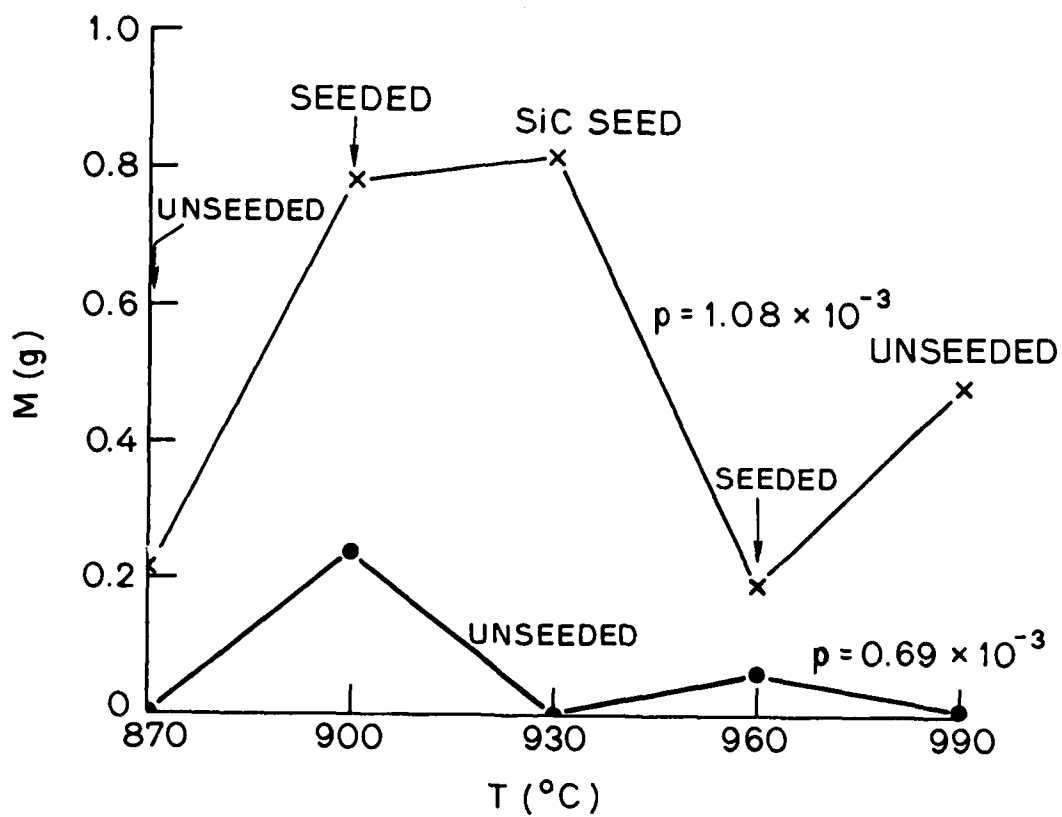


Fig. 6. Mass of GaN grown in compartmented crucible experiments as a function of temperature at various ammonia partial pressures.

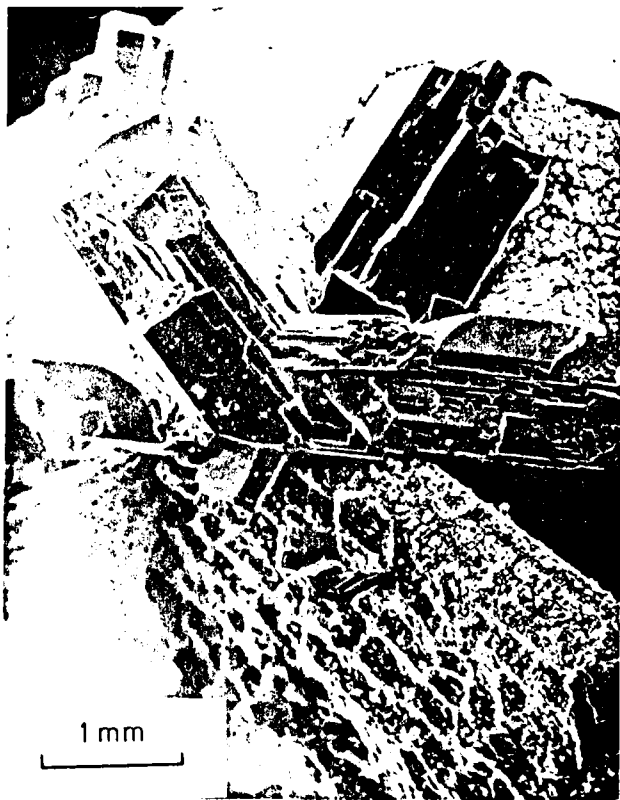


Fig. 7. Cluster of GaN crystals up to 2.5 mm long grown on SiC seed at 1.08×10^{-3} partial pressure at 930°C (20 X).

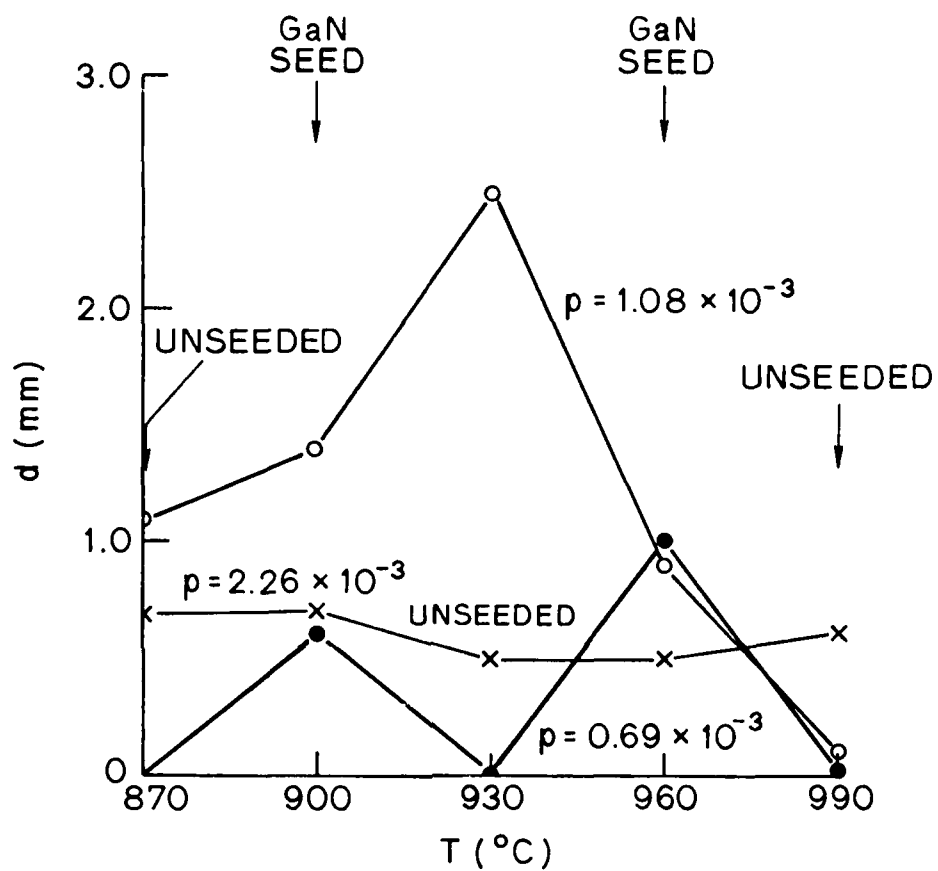


Fig. 8. Maximum crystal size versus temperature at various ammonia partial pressures.

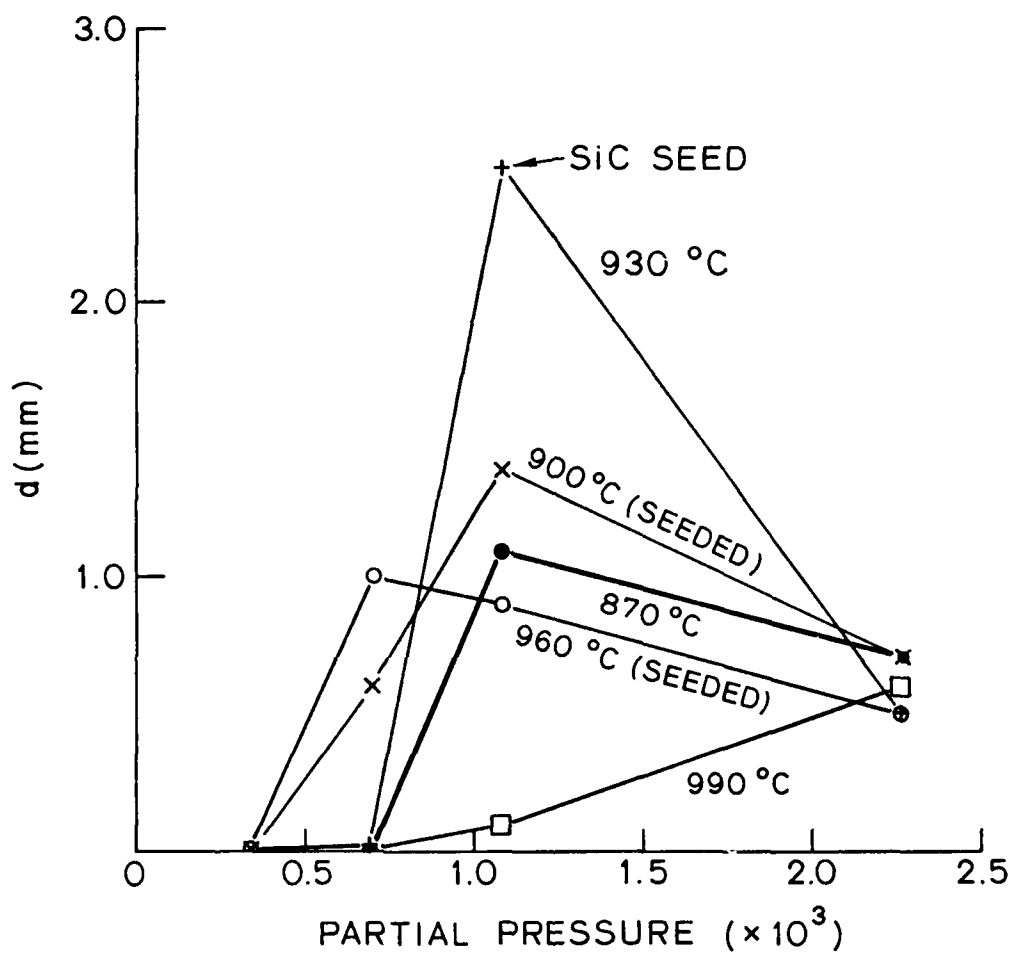


Fig. 9. Maximum crystal size versus ammonia partial pressure at different temperatures.

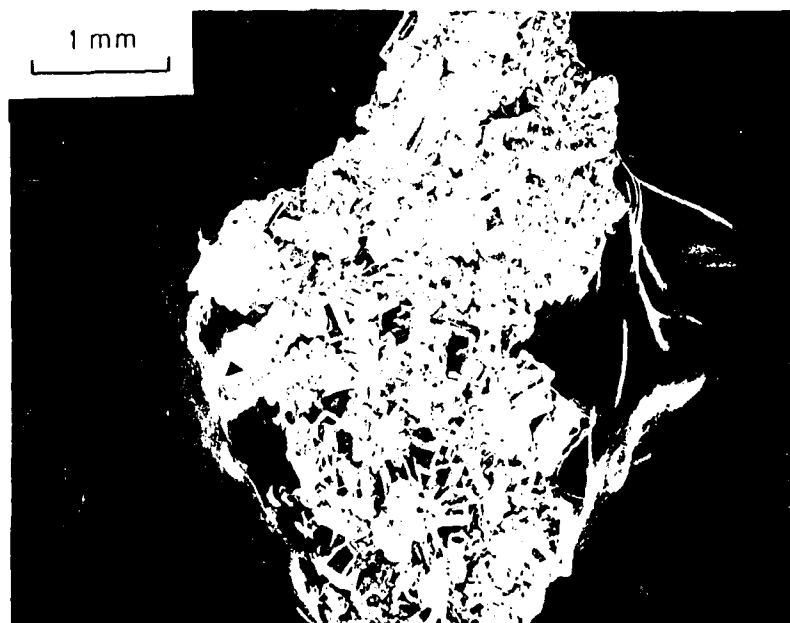
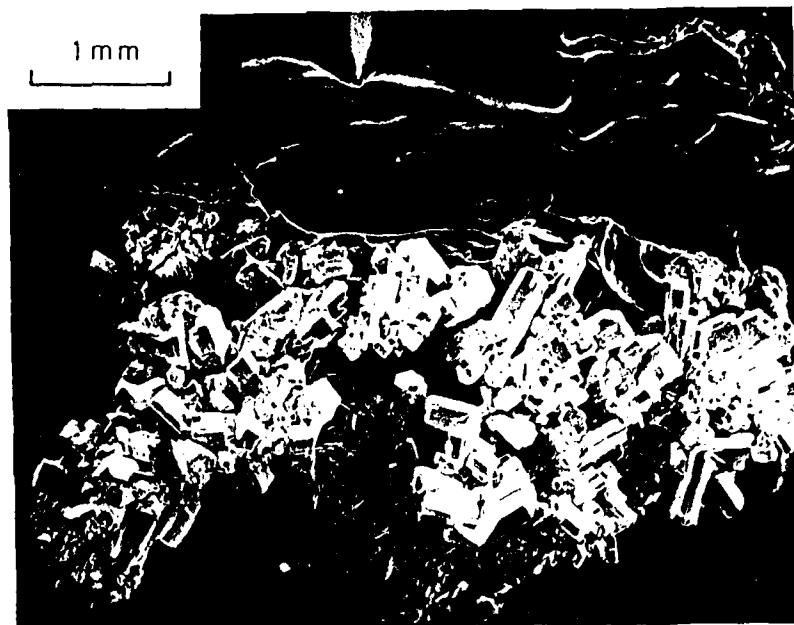


Fig. 10. Clusters of crystals (20 X) grown on seeds at 0.7×10^{-3} ammonia partial pressure (a) 900°C (b) 960°C .



Fig. 11. GaN crystal with {0001} face capped over (220 X).

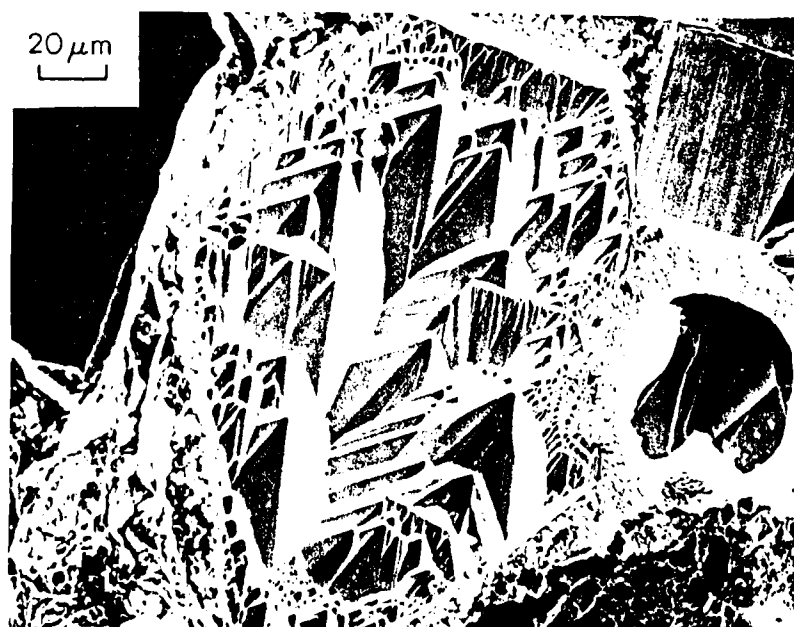


Fig. 12. GaN {0001} face with growth hillocks (500 X).

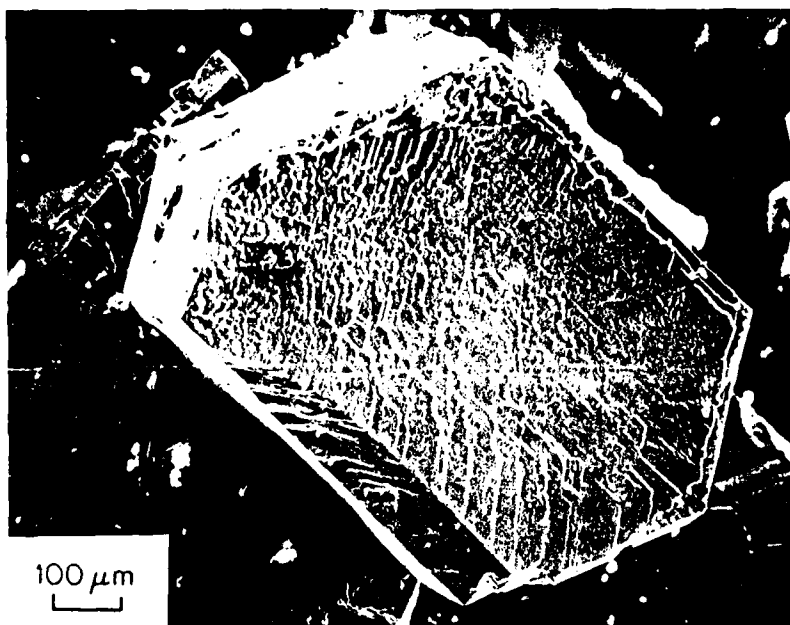


Fig. 13. GaN {0001} face with growth layers (100 X).

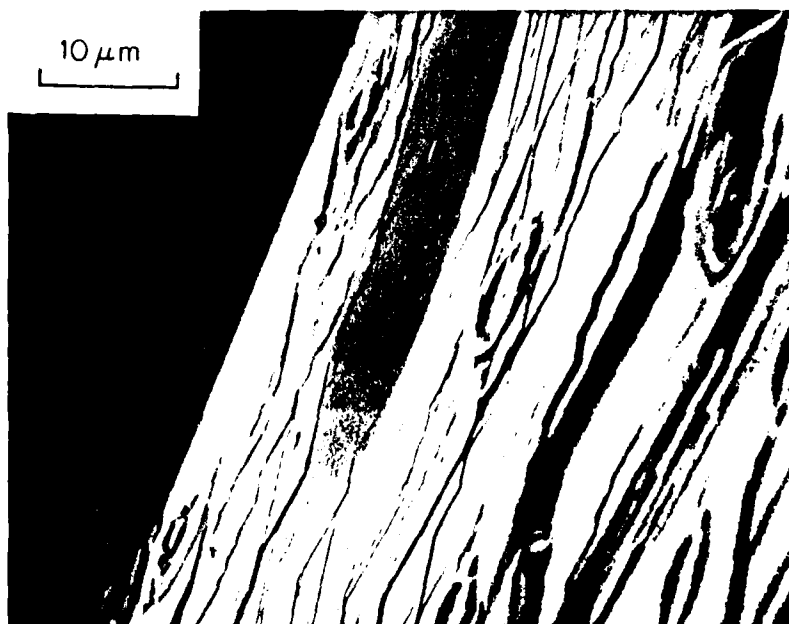


Fig. 14. GaN {1100} face with growth layers and islands which grew under Ga drops adhering to the layers after cooling (2000 X).

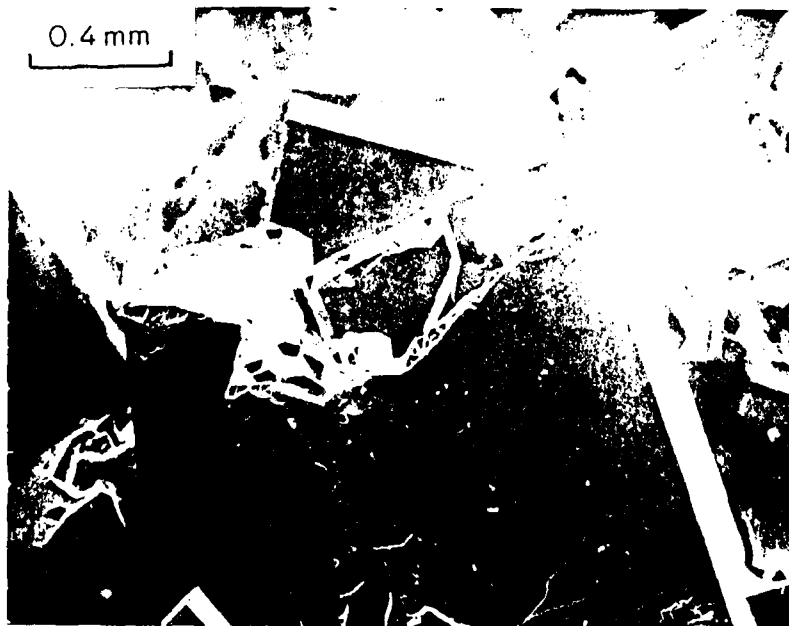
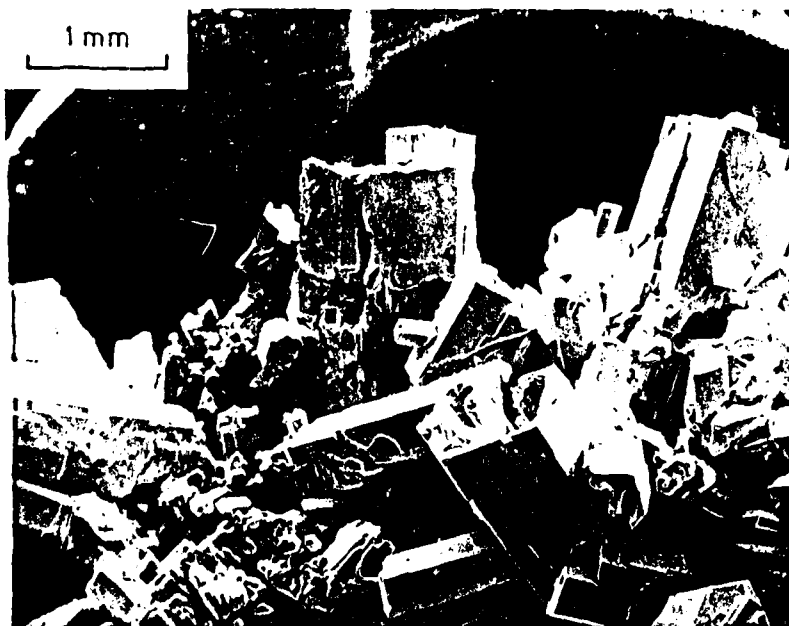


Fig. 15. (a) Cluster of hollow GaN crystals grown at 1.08×10^{-2} partial pressure and 900°C (20 X). (b) Magnified view of one hollow crystal (50 X).

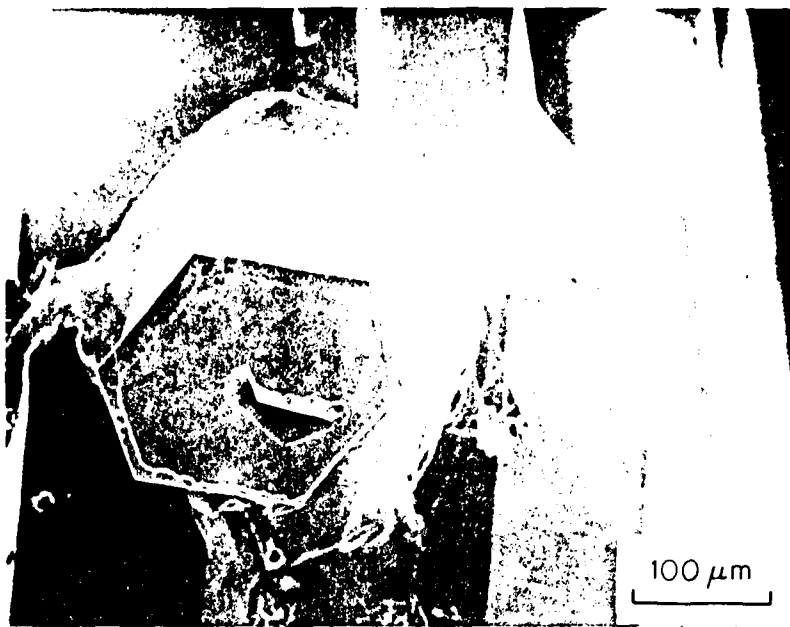


Fig. 16. (a) Small GaN crystal showing depression at face center (200 X).
(b) Larger crystal showing large, faceted central depression and subsidiary depressions (100 X).



Fig. 17. Light transmission through slice of GaN (310 X).

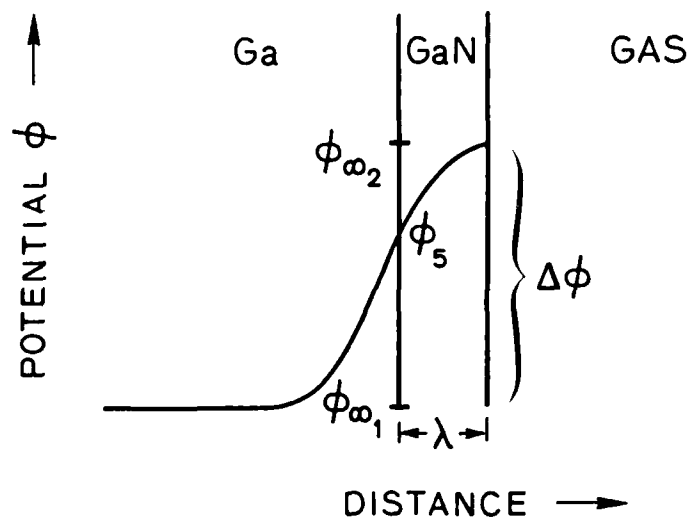
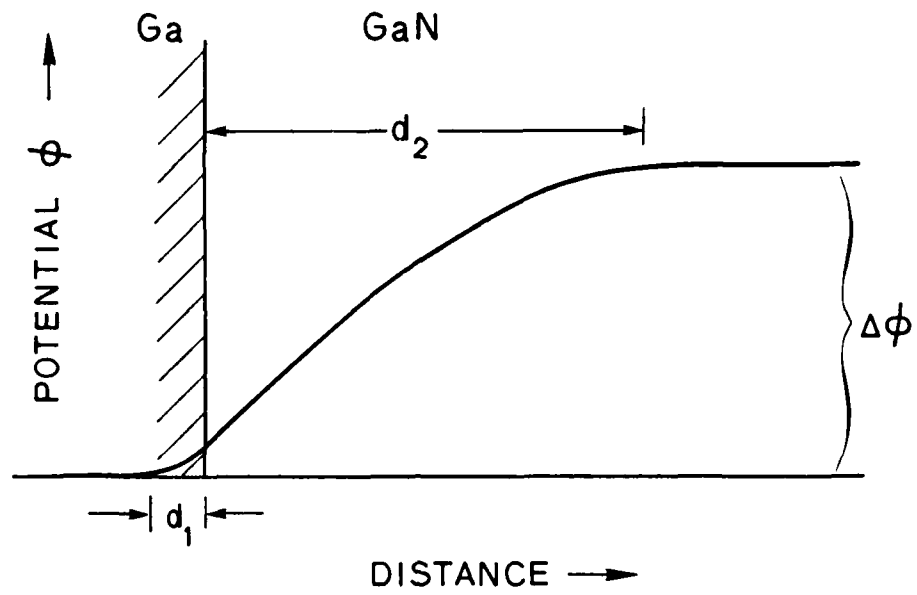


Fig. 18. Potential distribution across
 (a) Ga/GaN interface
 (b) thin GaN film.

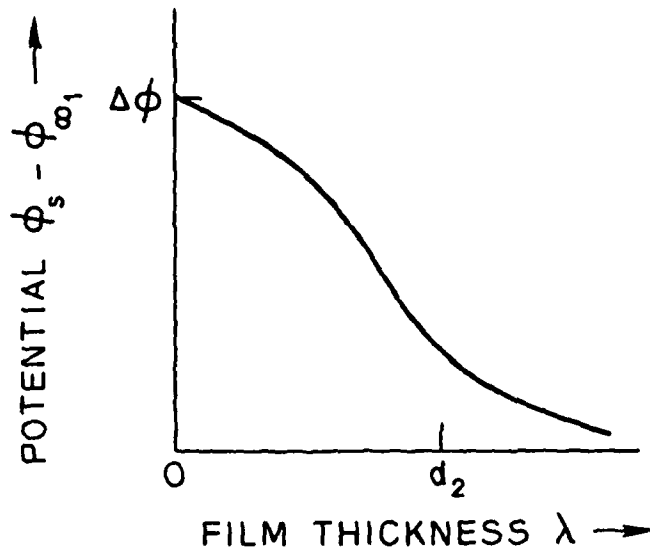


Fig. 19. Schematic variation of interface electrostatic potential with film thickness.

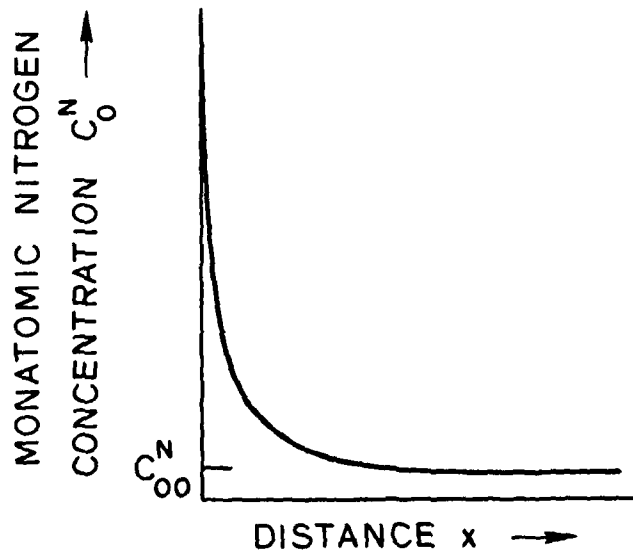


Fig. 20. Schematic variation of monatomic nitrogen concentration with distance x .

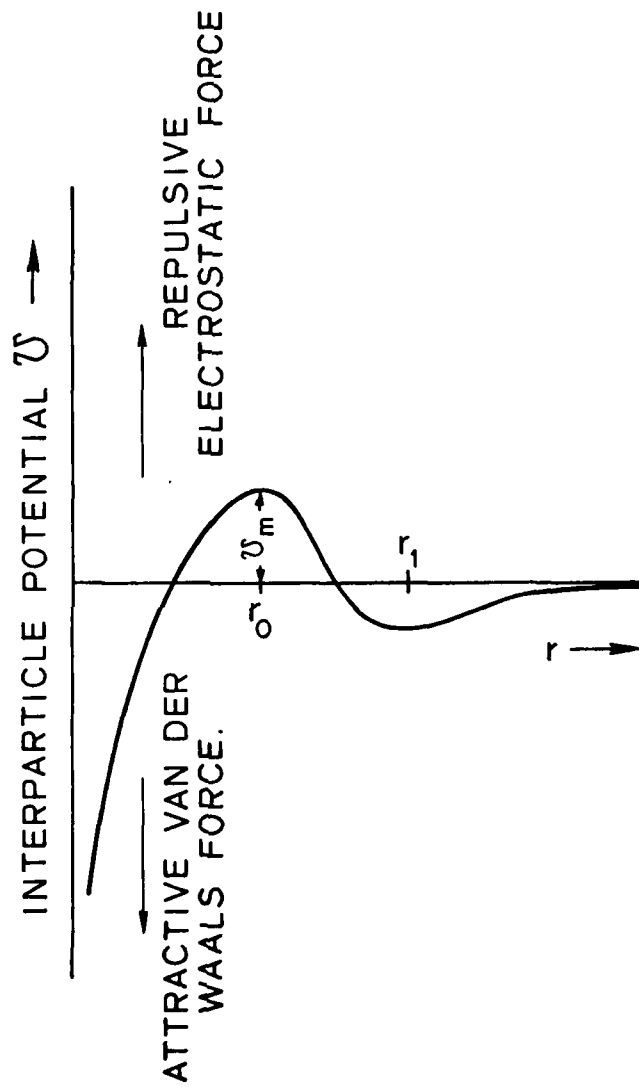


Fig. 21. Resultant of attractive van der Waals force and repulsive electrostatic force.